U.PORTO

FEUP FACULDADE DE ENGENHARIA
UNIVERSIDADE DO PORTO

Dissertation for Master's degree in Bioengineering

Biological Engineering Branch

Chitosan-engineered surfaces to prevent implant-associated infections

Marta Santos Lima

Supervisor: Dr. Rita T. Santos

Co-supervisors: Prof. Filipe J. M. Mergulhão and Dr. Luciana C. Gomes

Department of Chemical Engineering

Porto, July 5th 2021

“Não tenhamos pressa, mas
não percamos tempo.”

- José Saramago

Acknowledgements

Esta dissertação representa o culminar de mais uma etapa da minha vida, talvez a etapa mais incerta e desafiante de que tenho memória, o mestrado integrado em Bioengenharia. Ao longo destes 5 anos foram muitos os momentos de alegria, superação e concretização, mas também foram notórios os momentos de tristeza, incerteza e desmotivação. Foram esses momentos menos bons que me mostraram a energia, a força e a dedicação de alguns pilares fundamentais aos quais dedico este trabalho e sinto obrigação de agradecer.

Aos meus pais,

Por nunca terem desistido de mim e por me encorajarem sempre a seguir os meus sonhos, mesmo quando o caminho não é o mais fácil ou seguro. Agradeço-vos todo o amor, sacrifícios e incentivo.

À minha avó,

Por ter sido sempre o meu exemplo de fé e força. Agradeço-te todas as orações e inspiração. A confiança que sempre tiveste nas minhas capacidades, motiva-me diariamente a fazer mais e melhor.

À minha irmã,

Por ser, desde o primeiro dia, a minha grande companheira, a que estará ao meu lado em todas as jornadas da vida. Agradeço-te por me mostrares sempre o lado positivo de todas as situações, por acreditares mais em mim do que eu própria e por nunca me deixares satisfazer com o mínimo.

Ao Carlos,

Por ter sido sempre a minha maior força. Agradeço-te o companheirismo, a paciência, a persistência, o incentivo e o amor. Agradeço-te por teres acreditado sempre em mim e por teres estado sempre ao meu lado, nas alegrias e nas tristezas. Sem ti nada disto teria sido possível.

Aos meus orientadores,

Por toda a ajuda, dedicação e disponibilidade. Ao Professor Filipe Mergulhão, por todo o conhecimento e experiência. À Rita e à Luciana, por todos os conselhos, atenção, incentivo, otimismo e compreensão. Agradeço-vos, de coração, a enorme e incansável dedicação, em cada minuto deste projeto. Considero ter sido um privilégio poder fazer parte deste grupo de investigação.

Aos meus amigos de curso,

Por todas as memórias construídas aos longo destes anos. Em especial, agradeço à Sandra, à Bia e à Márcia pela amizade e por terem atenuado grande parte dos momentos menos bons. Foi um prazer poder fazer este percurso convosco.

À Faculdade de Engenharia da Universidade do Porto,

Por me ter me ter acolhido tão bem ao longo destes 5 anos. Agradeço à instituição pelo corpo docente de excelência e por ter contribuído para o meu crescimento intelectual e profissional.

Ao BEL (Biofilm Engineering Lab),

Por me ter fornecido as condições propícias à realização deste projeto de dissertação, com todo o material e equipamentos necessários.

Aos colegas dos laboratórios E-101 e E007,

Pelo ambiente acolhedor, pelo convívio e ajuda prestada. Em particular, agradeço à Ana, ao Fábio e à Marisa por todas as horas que perderam para me acompanhar ao tipo II e por toda a paciência.

Ao INL (International Iberian Nanotechnology Laboratory, Braga, Portugal) e ao IIM-CSIC (Instituto de Investigaciones Marinas, Vigo, Spain),

Pela produção e caracterização das superfícies à base de quitosano.

Às restantes pessoas,

Agradeço a todos que, de alguma forma, me ajudaram ao longo deste percurso.

Este trabalho foi financiado por: Financiamento Base - UIDB/00511/2020 da Unidade de Investigação - Laboratório de Engenharia de Processos, Ambiente, Biotecnologia e Energia – LEPABE - financiada por fundos nacionais através da FCT/MCTES (PIDDAC).











Abstract

Implantable medical devices (IMDs) are commonly used to ensure the patient's quality of life. However, these devices are prone to microbial adhesion and biofilm formation, leading to the development of implant-associated infections (IAIs). The antimicrobial resistance of biofilms has limited the strategies used to treat IAIs, which stresses the need to develop new biomaterials for the prevention and control of biofilm formation.

Chitosan (CS) is a natural polysaccharide that has been explored in the medical field due to its outstanding biological properties such as antimicrobial activity. Hence, the first part of the present work aimed to evaluate and critically discuss the anti-adhesive and antibiofilm activity of CS-based coatings to prevent IAIs through a systematic review of the literature following the PRISMA (Preferred Reporting Items for Systematic reviews and Meta-Analyses) guidelines. The second part of this project was focused on the study of the antimicrobial activity of CS-based surfaces against single- and dual-species biofilms of *Staphylococcus aureus* and *Pseudomonas aeruginosa*, as well as the effect of CS molecular weight (MW) on their antimicrobial activity. For this purpose, polylactic acid (PLA) surfaces immobilized with CS of different MW were used in biofilm assays, which were performed for 24 h under static conditions. Colony-forming unit (CFU) counts and epifluorescence microscopy were used to determine biofilm cell culturability and viability, respectively, while Confocal Laser Scanning Microscopy (CLSM) was used to analyze the biofilm structure and population distribution.

The systematic review indicated that the use of CS and CS associated with other compounds (antimicrobial peptides, enzymes, or polymers) is a promising approach to reduce biofilm formation on IMDs since they have a broad spectrum antimicrobial activity as well as the desirable properties for IMDs. Moreover, experimental results demonstrated that CS-based surfaces significantly reduced the biofilm formation, and their activity was dependent on MW since the surfaces with higher antibiofilm activity were those coated with the lowest MW CS. The immobilization of CS on PLA films reduced the number of total, viable, culturable and viable but non-culturable (VBNC) cells up to 80% for single-species biofilms of *S. aureus*, and up to 96% for single-species biofilms of *P. aeruginosa* and dual-species biofilms. The antibiofilm activity of CS-based surfaces was also corroborated by CLSM images and quantitative data.

Overall, these results suggest that CS can be a promising approach for the coating of IMDs since it efficiently reduced biofilm formation. Furthermore, the use of this natural polymer is a sustainable and eco-friendly strategy.

Keywords: Biofilm; Implantable Medical Devices; Chitosan; Molecular Weight; Antibiofilm surfaces

Resumo

Os dispositivos médicos implantáveis (DMI) são comummente utilizados para assegurar a qualidade de vida dos pacientes. No entanto, estes dispositivos são propensos à adesão microbiana e formação de biofilmes, levando ao desenvolvimento de infeções associadas a implantes (IAIs). A resistência antimicrobiana dos biofilmes tem limitado as estratégias utilizadas para tratar as IAIs, o que reforça a necessidade de desenvolver novos biomateriais para prevenir e controlar a formação de biofilmes.

O quitosano (em inglês, "chitosan" ou "CS") é um polissacarídeo natural que tem sido explorado na área médica devido às suas excelentes propriedades biológicas, tais como a atividade antimicrobiana. Assim, a primeira parte do presente trabalho pretendeu avaliar e discutir as propriedades anti-adesiva e antibiofilme dos revestimentos à base de CS para prevenir as IAIs, através de uma revisão sistemática da literatura orientada pela declaração PRISMA (Principais Itens para Reportar Revisões Sistemáticas e Meta-Análises). A segunda parte deste trabalho pretendeu avaliar a atividade antimicrobiana das superfícies à base de CS em biofilmes simples e mistos de *Staphylococcus aureus* e *Pseudomonas aeruginosa*, assim como o efeito do peso molecular do CS nas suas atividades. Para este propósito, superfícies de ácido polilático (em inglês, "polylactic acid" ou "PLA") imobilizadas com CS de diferentes pesos moleculares foram usadas em ensaios de biofilme, realizados durante 24 horas sob condições estáticas. A contagem de unidades formadoras de colónia e a microscopia de epifluorescência foram utilizadas para determinar a culturabilidade e a viabilidade das células do biofilme, respetivamente, enquanto a microscopia confocal (em inglês, "Confocal Laser Scanning Microscopy" ou "CLSM") foi usada para analisar a estrutura do biofilme e a distribuição das populações.

A revisão sistemática indicou que a utilização do CS e do CS associado a outros compostos (péptidos antimicrobianos, enzimas ou polímeros) é uma abordagem promissora para reduzir a formação de biofilme nos DMI, uma vez que estes têm uma atividade antimicrobiana de largo espetro, assim como outras propriedades desejáveis para estes dispositivos. Para além disso, os resultados experimentais demonstraram que as superfícies à base de CS reduziram significativamente a formação de biofilme e que a sua atividade foi dependente do peso molecular do CS, dado que as superfícies com maior atividade antibiofilme foram as revestidas com o CS de menor peso molecular. A imobilização de CS nos filmes de PLA reduziu o número de células totais, viáveis, cultiváveis e viáveis não cultiváveis (em inglês, "viable but non-culturable cells" ou "VBNCs") até 80% nos biofilmes simples de *S. aureus*, e 96% nos biofilmes simples de *P. aeruginosa* e biofilmes mistos das duas espécies bacterianas. A atividade antibiofilme das superfícies à base de CS foi também corroborada pelos resultados do CLSM.

Globalmente, estes resultados sugerem que o CS pode ser uma abordagem promissora para o revestimento dos DMI, uma vez que reduziu eficazmente a formação de biofilme. Para além disso, a utilização deste polímero natural é uma estratégia sustentável e amiga do ambiente.

Palavras-chave: Biofilme; Dispositivos Médicos Implantáveis; Quitosano; Peso Molecular; Superfícies Antibiofilme

Declaration

Declaro, sob compromisso de honra, que este trabalho é original e que todas as contribuições não originais foram devidamente referenciadas com identificação da fonte.

Declare, under oath, that this work is original and that all non-original contributions were properly referenced with the source identification.

July 5th, 2021 _____ Marta Santos Lima _____

(Marta Santos Lima)

Contents

Acknowledgements i
Abstract iii
Resumo iv
Declaration v
Contents vi
List of figures viii
List of tables x
Abbreviations xi
1. Introduction 1
1.1. Objectives 1
1.2. Relevance and motivation 1
1.3. Outline of the work 2
2. State of the art 3
2.1. Implantable medical devices 3
2.1.1. Implant-associated infections 3
2.2. Biofilms 4
2.2.1. Definition and formation 4
2.2.2. Biofilm on implantable medical devices 5
2.3. Chitosan 6
2.3.1. Definition and extraction 6
2.3.2. Properties and applications 7
2.3.3. Mechanism of action 7
3. Material and Methods 9
3.1. Systematic review 9
3.1.1. Search methodology, inclusion criteria and data extraction 9
3.2. Experimental work 10
3.2.1. Surface synthesis 10
3.2.2. Surface characterization 10
3.2.2.1. Water contact angle measurement 10
3.2.2.2. Fourier Transform Infrared Spectroscopy 10
3.2.2.3. Scanning Electron Microscopy 10
3.2.3. Bacteria and culture conditions 11
3.2.4. Biofilm assays 11
3.2.4.1. Biofilm formation 11

3.2.4.2. Cell supernatant analysis 12
3.2.4.3. Biofilm analysis 12
3.2.4.3.1. Colony-forming unit counts 12
3.2.4.3.2. Epifluorescence microscopy 12
3.2.4.3.3. Biofilm architecture by Confocal Laser Scanning Microscopy 13
3.2.5. Statistical analysis 14
4. Results and discussion 15
4.1. Systematic review 15
4.2. Experimental results 29
4.2.1. Characterization of synthesized surfaces 29
4.2.2. Cell supernatant analysis 30
4.2.3. Antibiofilm activity of PLA-CS surfaces 32
5. Conclusion 42
6. Outputs 43
7. Future perspectives 44
References 45
Appendices I
Appendix A – Supplementary material regarding systematic review I
Appendix B - Supplementary material regarding PLA and CS-coated PLA surfaces characterization III
Appendix C – Supplementary material regarding bacterial growth curves I
Appendix D - Supplementary material regarding the dual-species biofilms of *S. aureus* and *P. aeruginosa* V

List of figures

Figure 1. Main stages of biofilm development. 5

Figure 2. Schematic representation of chemical structure of (**a**) chitin and (**b**) chitosan. 6

Figure 3. Schematic representation of antimicrobial mechanisms of chitosan: cell membrane disruption, complexation with DNA and chelation of metals. 8

Figure 4. Flow of information through the different phases of a systematic review [54]. 9

Figure 5. Summary of the literature search based on the PRISMA flow-chart. 15

Figure 6. Colony-forming units counting of supernatant of (**a**) *S. aureus* and (**b**) *P. aeruginosa* after 24 h incubation with PLA, PLA-β-CS, PLA-CS1, PLA-CS2 and PLA-CS3 surfaces. Significant differences are considered for *p*-values < 0.05 and represented by *, ○, and □ when compared with PLA, β-CS, and CS1, respectively. 31

Figure 7. Cellular composition of 24-h single-species biofilms of (**a**) *S. aureus* and (**b**) *P. aeruginosa*, and of (**c**) dual-species biofilms of *S. aureus* and *P. aeruginosa* developed on PLA and CS-based surfaces: percentages of total, viable, culturable and viable but non-culturable (VBNC) cells of biofilms developed on β-CS, CS1, CS2 and CS3 surfaces compared to the control (PLA surfaces). Inferential statistics were performed using the nonparametric Mann-Whitney test and significant differences are represented for *p*-values < 0.05 by *, ○, □, and Δ when compared with PLA, β-CS, CS1, and CS2, respectively. 35

Figure 8. Representative biofilm structures of single-species biofilms of (**a-e**) *S. aureus* and (**f-j**) *P. aeruginosa* developed on PLA and synthesized CS surfaces. These images were obtained from CLSM *z*-stacks using IMARIS software and present an aerial, three-dimensional (3D) view of the biofilms (which vertical projections are represented by the shadow on the right). The scale bar is 50 μm. 39

Figure 9. Representative biofilm structures of dual-species biofilms of *S. aureus* and *P. aeruginosa* developed on PLA and synthetized CS surfaces. These images were obtained using IMARIS software and present an aerial view of biofilm structures (which vertical projections are represented by the shadow on the right). The first line (**i**) represents the combination of red and green filters (*S. aureus* + *P. aeruginosa* cells), while the second one (**ii**) corresponds only to the green filter (*S. aureus* cells on dual-species biofilms). The scale bar is 50 μm. 39

Figure 10. Biovolumes and thickness of (**a-b**) *S. aureus* and (**c-d**) *P. aeruginosa* single-species biofilms, and of (**e-f**) dual-species biofilms (*S. aureus* + *P. aeruginosa*) developed on PLA and synthesized CS surfaces. The values of these parameters were estimated from CLSM *z*-stacks using the COMSTAT2

tool associated with the ImageJ software, and the means ± standard deviations result from three independent assays. A one-way analysis of variance (ANOVA) was used to perform a statistical analysis and significant differences were represented for *p*-values < 0.05 by *, ○, □, and Δ when compared with PLA, β-CS, CS1, and CS2, respectively. 40

Figure A-1. Growth curves of (**a**) *S. aureus* and (**b**) *P. aeruginosa*. I

Figure A-2. Relation between $CFU.mL^{-1}$ and $OD_{610\ nm}$ for (**a**) *S. aureus* and (**b**) *P. aeruginosa*. I

Figure B-1. Number of published studies about the anti-adhesive and/or antibiofilm activity of chitosan with application in implantable medical devices, per year. II

Figure C-1. Representative images of water contact angles on (**a**) PLA and CS-coated PLA surfaces: (**b**) PLA-β-CS; (**c**) PLA-CS1; (**d**) PLA-CS2; and (**d**) PLA-CS3. III

Figure C-2. FTIR spectrum of PLA films and PLA films immobilized with different samples of chitosan: β-CS, CS1, CS2, and CS3. III

Figure C-3. SEM images of PLA films (**a**) and PLA films immobilized with the highest (**b,** β-CS) and lowest (**c**, CS3) molecular weight chitosan, with a magnification of 500x. IV

Figure D-1. Proportion of *S. aureus* (■) and *P. aeruginosa* (■) (**a-e**) culturable cells and (**f-j**) biovolume in dual-species biofilms formed on PLA and CS-coated PLA surfaces. V

Figure D-2. Representative CLSM image of the co-localization of *P. aeruginosa* and *S. aureus* along the vertical (*z*) position in dual-species biofilms formed on CS-based surfaces. Scale bar corresponds to 50 μm. V

List of tables

Table 1. Studies reporting the anti-adhesive and/or antibiofilm efficacy of chitosan and functionalized chitosan..... 20

Table 2. Studies reporting the efficacy of coatings based on chitosan associated with antimicrobial compounds. 23

Table 3. Studies reporting the efficacy of coatings based on chitosan associated with metals. 26

Table 4. Studies reporting the efficacy of coatings based on chitosan associated with polymers. 28

Table C-1. Water contact angles (mean ± SD) of PLA and PLA-CS films developed by dip-coating method. III

Abbreviations

CFU – Colony-Forming Unit

CLSM – Confocal Laser Scanning Microscopy

CS – Chitosan

EPS – Extracellular Polymeric Substances

FTIR – Fourier Transform Infrared Spectroscopy

IAIs – Implant-Associated Infections

IMDs – Implantable Medical Devices

LB – Luria-Bertani

MINORS – Methodological Index for Non-Randomized Studies

MW – Molecular Weight

OD – Optical Density

PLA – PolyLatic Acid

PRISMA – Preferred Reporting Items for Systematic reviews and Meta-Analyses

PI – Propidium Iodide

QS – Quorum Sensing

SEM – Scanning Electron Microscopy

SD – Standard Deviation

UV – Ultraviolet

VBNC – Viable But Non-Culturable

1. Introduction

1.1. Objectives

Implantable medical devices (IMDs) are associated with several clinical complications, including the occurrence of infections, since they are very prone to microbial adhesion and, consequently, biofilm formation [1]. Despite the recent advancements in material science, the incidence of implant-associated infections (IAIs) has significantly increased, being an economic and social burden [2]. The resistance of established biofilms to antimicrobial therapies poses serious clinical challenges and has led to a continuous pursuit for effective strategies to inhibit or control biofilm formation, such as the development of new biomaterials with anti-adhesive and antibiofilm properties. In the last years, chitosan (CS) has been widely used in the medical field due to its biological features, including high antimicrobial activity [3]. Considering the antimicrobial properties of this natural polymer and the high incidence of IAIs, this study aimed to evaluate the anti-adhesive and antibiofilm activity of CS-based surfaces for application in IMDs.

For this purpose, the first aim of this work was to systematically review the literature concerning the use of CS alone or in association with other compounds to prevent or control microbial adhesion and biofilm formation on IMDs, using the Preferred Reporting Items for Systematic reviews and Meta-Analyses (PRISMA) method.

The second aim of this work consisted of evaluating the physicochemical properties and morphology of CS-based surfaces produced by immobilization of CS of different molecular weights (MW) on polylactic acid (PLA) films, and testing their ability to inhibit or reduce single- and dual-species biofilm formation by *Staphylococcus aureus* and *Pseudomonas aeruginosa*, two common bacteria isolated from IAIs [4]. In addition, the effect of MW on CS antimicrobial and antibiofilm activity was also evaluated. CS-based surfaces were characterized by contact angle measurements, Fourier Transform Infrared Spectroscopy (FTIR), and Scanning Electron Microscopy (SEM). In turn, biofilms were developed in 12-well microtiter plates containing PLA films (control surface) and four CS-based surfaces with decreasing MWs (β-CS, CS1, CS2, and CS3). Subsequently, the number of total and viable cells was determined by epifluorescence microscopy using the Live/Dead kit, whereas the number of culturable cells was determined by colony-forming units (CFU) count. Moreover, biofilm spatial distribution was analyzed by Confocal Laser Scanning Microscopy (CLSM).

1.2. Relevance and motivation

IAIs are mostly caused by the development of biofilms on implant surfaces. Biofilm resistance has limited the efficacy of antimicrobial treatments, contributing to an increase of IAIs' incidence which currently reaches 40% [2]. These infections represent a social and economic burden, since they are

responsible for prolonged hospital stays, increased costs, and high morbidity and mortality rates [5]. For this reason, it is imperative to find novel approaches to reduce the occurrence of IAIs.

In the last years, some strategies have been proposed to reduce bacterial adhesion and biofilm formation through the modification of surface topography and chemistry of implant material [6]. The current strategies used to prevent bacterial adhesion are essentially based on coating IMDs with compounds that generate anti-adhesive/bacteria-repelling (e.g., polymers), contact-killing (e.g., antimicrobial peptides), or antimicrobial-releasing (e.g., metals and biocides) surfaces [7, 8]. However, despite the efforts to reduce the incidence of IAIs, most of the developed coatings exhibit low biocompatibility (e.g., polymers) and high toxicity for human cells (e.g., antimicrobial peptides may be toxic at high doses) and can lose their properties when implants are used for long-term periods (e.g., antimicrobial agents) [9]. Moreover, the antimicrobial efficacy of these compounds has not been completely proven and most of them may trigger microbial resistance [9].

Therefore, the novelty of this work consists of using CS isolated from *Loligo opalescens* squid endoskeletons and its derivatives of different MW to produce CS-based surfaces with antimicrobial activity that could be applied as antibiofilm coatings on IMDs. Besides CS antimicrobial activity against a broad spectrum of microorganisms, this semi-natural polymer has attracted considerable attention due to its biocompatibility, biodegradability, and non-toxicity [3], being a promising alternative that may overcome the limitations of current strategies. Furthermore, CS extraction is an economically and eco-friendly process [10] with important implications for the circular economy.

1.3. Outline of the work

The present thesis contains seven sections. Section 1 consists of an introductory chapter where the theme of the work is contextualized, the objectives are listed, and the motivations and relevance of the work are presented. In Section 2, the state of the art is presented and the concepts relevant to the work are explained. The literature review is structured as follows: i) introduction to IMDs and problems associated with their use, namely the occurrence of IAIs, ii) description of the biofilm formation process and its implications on IMDs, iii) and introduction of CS and characterization of its main properties and mechanism of action. Sections 3 and 4 are divided into two sub-sections: the systematic review and experimental work. Section 3 shows the materials and methodologies used in this work, while Section 4 presents the obtained results and their discussion. In turn, Section 5 presents the main conclusions of this work. Finally, Sections 6 and 7 list the outputs of this work and suggestions for future studies, respectively.

2. State of the art

2.1. Implantable medical devices

IMDs can be defined as any devices that are inserted into the human body for a short or long period to support, replace or repair some biological structure (e.g., bone, hip, joint, breast, pelvis, teeth, and others) that was damaged or lost [7, 11, 12]. IMDs have been used in the medical field for both diagnosis and therapeutic purposes [12, 13] and can be divided into three classes according to their application: orthopedic implants, such as bone cement, hip replacement implants, cervical implants, and internal fixation devices; cardiovascular implants, including pacemakers, coronary stents, heart valves, and implantable cardioverter defibrillators; and other medical implants, such as otolaryngol implants (e.g., cochlear implants), ophthalmic implants (e.g., intraocular lenses), gastroenterological implants (e.g., gastric bands), gynecological devices (e.g., intrauterine devices), and drug implants [7, 12, 13].

IMDs are commonly made from metals, polymers, and ceramics. Although many metals and ceramics are used for implant production, their use is limited since metals are associated with corrosion, stress protection, and wear and debris formation, which lead to the necessity of implant replacement, while ceramics have poor fracture toughness [13]. Consequently, these materials have been replaced by polymeric matrices, such as polylactic acid (PLA), due to their versatility, availability, biodegradability, biocompatibility, and non-toxicity, which are properties desirable for IMDs [11].

In the last years, the aging population, the growing occurrence of comorbidities and deteriorating lifestyle have increased the number of implanted medical devices [12, 13]. In the United States, more than 3.6 million implants are annually inserted [14] and the active IMDs market was valued at over $7.49 billion in 2020 and forecasted to reach $10.77 billion by 2025, at a compound annual growth rate of 7.53% [15].

Although IMDs are essential for ensuring the patients' quality of life, all these medical devices are susceptible to microbial colonization [16], leading to the occurrence of IAIs [1].

2.1.1. Implant-associated infections

Despite the careful aseptic handling and the effort to maintain their sterility, IMDs are foreign surfaces in the human body that can be easily colonized by pathogens, leading to the development of IAIs. These infections can occur due to bacterial contamination of the surgical site during surgery or in the moments afterward, by the spread of pathogenic microorganisms through the bloodstream from a distant focus of infection, or by direct spread from an infectious focus near the implanted device [17]. Moreover, IAIs can be classified as early, delayed, or late infections, depending on the post-surgery period in which they develop. In prosthetic joints, early infections occur during the first 3 months and are mainly caused by virulent microorganisms (e.g. *S. aureus*), while delayed and late infections occur

3-24 months and more than 24 months after surgery, respectively, and are commonly caused by low-virulence microorganisms, such as those typically found in normal skin flora [4, 17].

IAIs have an incidence between 2-40%, depending on the type of implanted medical device [2], and are responsible for longer hospital stays and increased hospital costs [5]. In the United States, these infections account for about 60-70% of the 2 million healthcare-associated infections reported annually [16, 18], and represent approximately $3 billion of direct costs [19]. Moreover, IAIs are responsible for high mortality rates, which are highly dependent on implanted devices. Devices such as joint prosthetics and mammary implants are associated with a mortality rate lower than 5%, while heart assist devices are associated with mortality rates above 25% [5].

The susceptibility and severity of IAIs could also be associated with some characteristics of the patient (e.g., age, comorbidities and immune defenses), operative procedures (e.g., type of procedure and surgeon´s experience), implantable devices (e.g., nature of implant) and etiological agent [12]. However, it is known that IAIs are mainly caused by microbial adhesion and biofilm formation on implant surfaces [2].

2.2. Biofilms

2.2.1. Definition and formation

The microorganisms living in nature can switch between a planktonic and a sessile state. More than 90% of microorganisms are in a sessile state due to variations in environmental conditions that lead them to organize into microbial communities called microbial biofilms [20, 21]. Biofilm formation proceeds the adhesion of microorganisms to a wide variety of surfaces, where occurs cellular division and, consequently, surface colonization. Biofilms can be defined as complex agglomerates of microorganisms, living in an organized, structured, and three-dimensional community, that is surrounded by a self-produced matrix of extracellular polymeric substances (EPS) [9]. This matrix protects sessile microorganisms from external environmental conditions (e.g., mechanical or physical stress, human defenses, and antimicrobial drugs) and is usually composed of exopolysaccharides, nucleic acids, lipids, and proteins that support the attachment to the surface [22]. Other noncellular compounds, including corrosion particles, mineral crystals, and clay or silt particles can be found in biofilm composition [23].

Biofilm formation is a dynamic process that usually involves some consecutive steps as represented in Figure 1. In the first stage, planktonic cells are transported to the surface through physical forces or bacterial appendages (e.g., flagella or pili) [24]. Then, the first microorganisms adhere to the surface via Van der Waals forces, electrostatic interactions, steric interactions, and hydrophobic interactions. The initial interaction between the microorganisms and the surface is weak and reversible and depends on some environmental conditions, such as pH, temperature, exposure time, and surface treatment [25]. After that, the irreversible attachment stage occurs and the microorganisms' appendages

overcome the physical repulsive forces and anchor on the surface, immobilizing the reversibly attached microorganisms. Subsequently, microorganisms start to produce the extracellular polymeric matrix that involves individual cells, forming the biofilm [26]. At this level, the biological contribution of microorganisms becomes more significant than physical and chemical processes. Microorganisms begin to produce autoinducer signals which allow them to communicate with each other via quorum sensing (QS). Then, the biofilm progressively spreads over the surface by exponential growth of its population, achieving maturation. This process depends on the substrate, pH, and oxygen concentrations [25]. In the last stage, biofilm cells detach and leave the biofilm cavities and are transported by the bulk fluid, colonizing new areas [27].

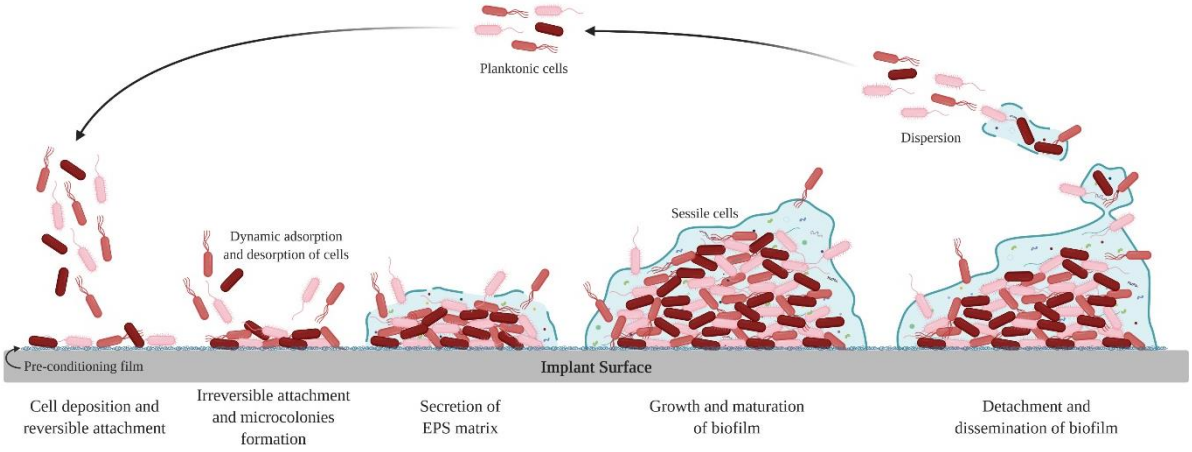


Figure 1. Main stages of biofilm development.

2.2.2. Biofilm on implantable medical devices

Most of IMDs are susceptible to microbial adhesion and, consequently, biofilm formation, which is the leading cause of IAIs. Depending on the type of implantable device and the anatomical site of implantation, device-related infections can be caused by a variety of pathogens [18, 28]. The most common microorganisms responsible for IAIs are *Staphylococcus* spp., *Staphylococcus epidermidis* and *Staphylococcus aureus*, being responsible for about 40-50% of prosthetic heart valve-related infections and 50-70% of catheter-related infections [4, 7, 29]. Other pathogens isolated from implantable devices include *Enterococcus* spp., *Candida* spp., *Escherichia coli*, *P. aeruginosa*, and *Klebsiella* spp., especially in infections associated with intravascular devices, prosthetic joints, and urinary tract devices [12, 18].

Once adhered to inert implant surfaces, these pathogens can rapidly form biofilms which protect them against hostile environmental conditions, host immune responses, and antimicrobial agents [30, 31], hampering the prevention, diagnosis, and treatment of IAIs [7]. In fact, microorganisms living in a biofilm community can be 1000-times more resistant to antimicrobial treatment than their planktonic counterparts [32]. Biofilm resistance may be related to the EPS matrix production (that forms a barrier that difficult antimicrobial agents penetration), the reduced growth rate of microorganisms within the

biofilm [4], and the presence of persister cells that remain in a dormant state but can regrowth and be responsible for reinfections [33, 34].

The current treatment of IAIs often requires long-term antibiotic therapies with high-dose antibiotics depending on the severity of infection [7]. However, the increasing antimicrobial resistance has difficulted the prevention and control of biofilm formation and the traditional strategies used to fight planktonic cells have been ineffective against biofilms [32]. Hence, the pathogens within the biofilm can resist antibiotic action and the infection can persist until the implant is removed [35]. The removal of an infected device and implantation of a new one requires high-risk and expensive surgeries [7, 36].

The consequences of IAIs may include prolonged hospitalization with antibiotic therapy, device failure, chronic infections, and even amputation [7, 29]. Since these infections pose serious threats to public health, it is essential to design new approaches to prevent and control IAIs, such as the development of improved antimicrobial coatings.

2.3. Chitosan

2.3.1. Definition and extraction

CS is a semi-natural cationic polymer obtained from chitin (Figure 2), which is the second most abundant natural amino polysaccharide after cellulose [10]. This plentiful resource composed of 2-acetamide-2-deoxy-d-glucopyranose units linked by β-(1-4) bonds is commonly extracted from exoskeletons of crustacean shells, molluscs and insects, and cell walls of fungi [37]. Depending on the source used to extract chitin, it can have two configurations, α-chitin and β-chitin. The insolubility of chitin in water and most organic solvents limits its use and encourages its conversion into CS through its partial N-deacetylation using alkaline hydrolysis or enzymatic methods [21, 38]. CS obtained is a polysaccharide consisting of β-(1-4)-linked N-acetyl-*D*-glucosamine and *D*-glucosamine units, soluble in most acid solutions at pH bellow 6.5 due to the quaternization of amino groups with a pKa ~ 6.3.

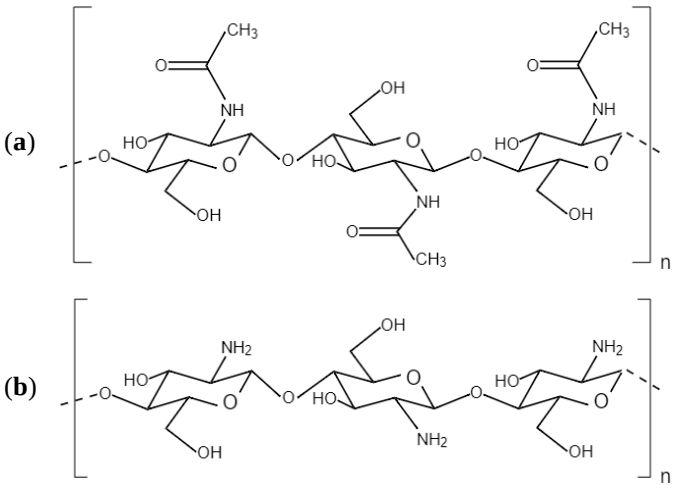


Figure 2. Schematic representation of chemical structure of (**a**) chitin and (**b**) chitosan.

Besides being a very abundant resource, the use of chitin and CS can be advantageous in solving some environmental problems. In the last few decades, squid pens are a source of chitin that is increasingly explored [39]. The number of squid captures reached 4 million tonnes in 2015 [40]. Considering that the average yield of edible flesh in squid is only 70%, squid processing produces a substantial amount of waste that ranges from 0.8 to 1.6 million tonnes per year [41, 42]. Therefore, to avoid the costly disposal of this waste and in order to enhance the potential of chitin and CS valorization, the concept of shell biorefinery was suggested [40]. This concept aims to benefit both the economy and the environment field through the sustainable conversion of chitin and CS into nitrogen-rich chemicals for various applications (e.g. pharmaceuticals, cosmetics and water treatment) [40, 43].

2.3.2. Properties and applications

In the last years, CS has been introduced in the medical field due to its outstanding intrinsic properties, namely high biocompatibility, biodegradability, low allergenicity, and low toxicity for human cells [3]. Furthermore, CS and its derivatives have a wide spectrum of antimicrobial activity against Gram-positive and Gram-negative bacteria, filamentous fungi, and yeasts, both in planktonic and sessile states [44], being very attractive materials for the design of antimicrobial coatings for medical applications. This polymer can be prepared in different formulations, such as nanoparticles, gels, fibers, membranes, or sponges, allowing a large variety of medical applications such as wound healing [45], tissue engineering [46], skin regeneration [47] or drug delivery [48].

2.3.3. Mechanism of action

Although the CS mechanism of action is not entirely known, three main mechanisms were proposed for the inhibition of microbial growth (Figure 3): i) cell membrane disruption, ii) complexation with DNA, and iii) chelation of metals. The first mechanism is based on electrostatic interactions between the positively charged CS molecules (due to the NH_3^+ amino groups of glucosamine) and negatively charged cell membranes (due to the presence of phospholipids with anionic phosphate groups). These interactions lead to changes in the permeability of cell membranes with consequent loss of intracellular content and cell death [49, 50]. The second mechanism consists of the interaction of diffused hydrolysis products with microbial DNA. The penetration of CS into microbial cells and its binding to DNA molecules result in the inhibition of mRNA and protein synthesis [51]. In the third mechanism, CS molecules can chelate with some metal ions (e.g., Ca^{2+} and Mg^{2+}), damaging the integrity of the microbial cell walls [49, 52].

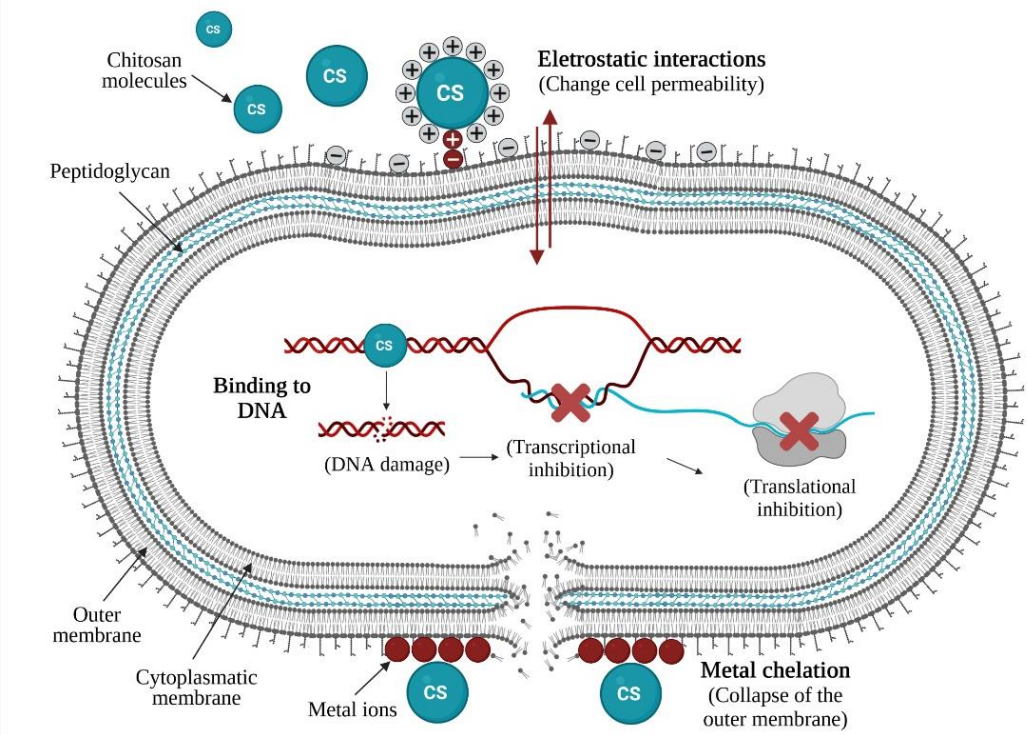


Figure 3. Schematic representation of antimicrobial mechanisms of chitosan: cell membrane disruption, complexation with DNA and chelation of metals.

The antimicrobial properties of CS and its derivatives are dependent on a set of environmental parameters, such as the pH, microorganism species, and CS structural properties such as MW, degree of deacetylation, concentration, and source [49, 53]. In addition, depending on environmental conditions, the CS antimicrobial activity may result from the combination of different mechanisms, which hinders the development of microbial resistance, making CS a promising biopolymer for coating IMDs.

3. Material and Methods

3.1. Systematic review

3.1.1. Search methodology, inclusion criteria and data extraction

A systematic review was conducted following the Preferred Reporting Items for Systematic reviews and Meta-Analyses (PRISMA) statement guidelines [54] to explore the antimicrobial and anti-adhesive potential of CS-based coatings for application in IMDs. The search method is based on a four-phase flow diagram (Figure 4), which is complemented by a 27-item checklist [54].

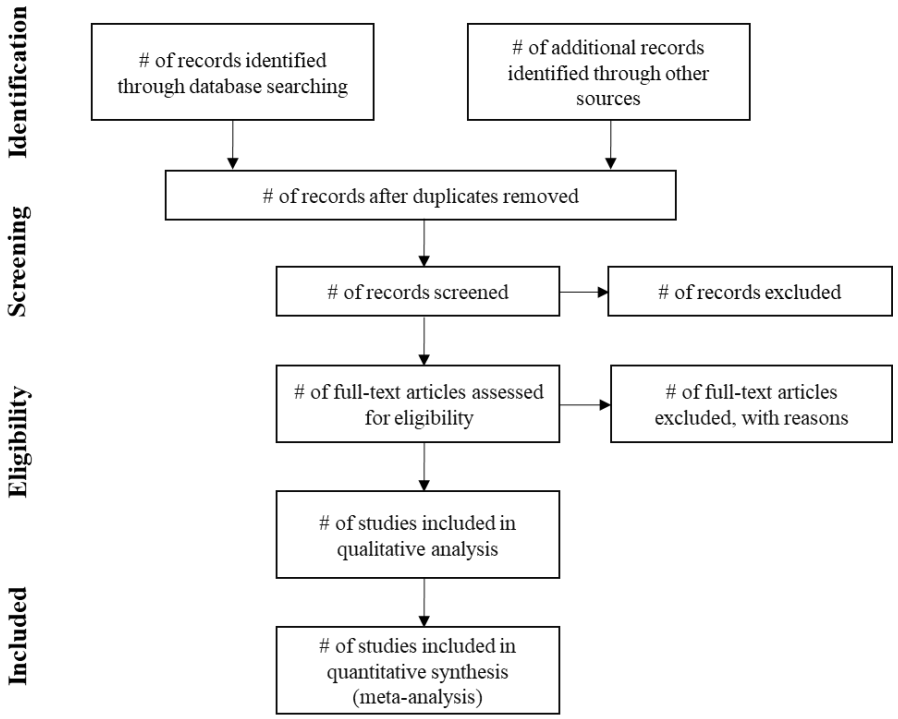


Figure 4. Flow of information through the different phases of a systematic review [54].

The search was performed until 1st April 2021 in PubMed, Cochrane, Compendex, and Scopus libraries through the combination of the following keywords “chitosan”, “medical applications”, “antimicrobial”, “antibiofilm”, “biofilm”, and “adhesion”. Full-text manuscripts published since January 2000 were assessed for eligibility. The adopted inclusion criteria were i) studies that used CS to reduce microbial adhesion and/or biofilm formation on the surfaces of IMDs, ii) studies focused on the antimicrobial and anti-adhesive effects of CS in association with other compounds for application in IMDs, and iii) original articles. The exclusion criteria consist of articles that did not perform adhesion or biofilm assays.

After the screening, the studies selected for full revision (eligible studies) were analyzed and the information about study design, CS composites, surface materials, medical applications, tested microorganisms, used methodologies, and major conclusions were registered.

3.2. Experimental work

3.2.1. Surface synthesis

CS used in this study was isolated from the *Loligo opalescens* squid pens through a combination of enzymatic and alkaline treatments [55] by Grupo de Reciclado y Valorización de Materiales Residuales (REVAL) from Instituto de Investigaciones Marinas (IIM-CSIC, Spain). From this procedure, a highly purified CS (β-CS) with a MW of 294 kDa was obtained and submitted to a depolymerization reaction [56] to produce three CS of different MW: CS1 of 186 kDa, CS2 of 129 kDa, and CS3 of 61 kDa. Subsequently, 0.5% (w/v) CS solutions were immobilized on PLA films (1 cm × 1 cm) by dip-coating [57] by International Iberian Nanotechnology Laboratory (INL, Braga). PLA was the selected substrate since this material is commonly used for implant production [58, 59].

3.2.2. Surface characterization

INL carried out a characterization of PLA and PLA films immobilized with CS by evaluating the wettability of the surfaces, the intermolecular interactions between the PLA and the CS, and the morphology of the synthesized surfaces.

3.2.2.1. Water contact angle measurement

To evaluate the hydrophobicity of the synthesized surfaces, the water contact angle was measured by the sessile drop method using a drop shape analysis system (DSA 100E, Kruss Gmbh, Germany). A 2 µL water droplet was placed in different positions of the tested surfaces and drop images were recorded using a digital camera connected to the analyzer. From these images, the circle fitting method was used to estimate the contact angle. A minimum of 10 measurements was performed for each tested surface.

3.2.2.2. Fourier Transform Infrared Spectroscopy

The intermolecular interactions between the CS and the PLA films were evaluated by Fourier Transform Infrared Spectroscopy (FTIR). FTIR spectra of the produced PLA-CS surfaces were recorded with VERTEX 80v FTIR spectrometer (Bruker, Germany) in the wavelength range 4000-400 cm^{-1} at a resolution of 4 cm^{-1} and normalized between 0 and 1, using Platinum Attenuated Total Reflection (ATR) mode (Bruker, Germany).

3.2.2.3. Scanning Electron Microscopy

A Scanning Electron Microscope (SEM; Quanta 650 FEG, FEI, USA) was used to study the morphology and the distribution of CS and its derivatives on PLA films. For that, samples were cut,

placed on sample holders with double-sided adhesive tape, and sputtered with a 10 nm layer of gold. After that, the samples were observed in SEM with an accelerating voltage of +5 kV at 500 ×.

3.2.3. Bacteria and culture conditions

To evaluate the antibiofilm activity of the synthesized surfaces, *Staphylococcus aureus* ATCC 25923 and mCherry-*Pseudomonas aeruginosa* PAO1 were selected since they are representative model strains of pathogenic bacteria responsible for IAIs [4]. Bacteria preserved at -80 ºC in Luria-Bertani (LB) broth (Thermo Fisher Scientific, USA) containing 20% (v/v) glycerol were spread on Plate Count Agar (PCA, Merck KGaA, Germany) plates and incubated for 24 h at 37 ºC. Single colonies were collected from agar plates, inoculated in 50 mL of LB medium and incubated overnight (16 ± 2 h) at 37 ˚C with orbital shaking (160 rpm; New Brunswick™ Innova® 44 shaker, Eppendorf AG, Germany). A tetracycline solution at 1.25 $g.L^{-1}$ was used to select mCherry-*P. aeruginosa* colonies. LB is a bacterial cell culture medium (composed of tryptone, yeast extract and NaCl) that is widely used since it allows the fast growth of many pathogenic bacteria [60]. The overnight cultures were then harvested by centrifugation (Eppendorf Centrifuge 5810R, Germany) at 18 ˚C, 3202 *g*, for 10 min. After resuspending the pellet in fresh LB medium, the cellular suspensions were adjusted to an optical density at 610 nm ($OD_{610\ nm}$) of 0.10, which corresponds to a final bacterial concentration of approximately 1×10^7 $CFU.mL^{-1}$ (Figure A-2 in Appendix A), representative of a real clinical situation [61]. Bacterial suspensions of *S. aureus* and *P. aeruginosa* were directly used for single-species biofilm formation assays, while for dual-species biofilms the bacterial suspensions were mixed in a 1:1 ratio.

3.2.4. Biofilm assays

3.2.4.1. Biofilm formation

Biofilm assays were performed on 12-well microtiter plates (VWR International, Carnaxide, Portugal) under static conditions and carried out on PLA (positive control) and four synthesized CS surfaces (PLA-β-CS, PLA-CS1, PLA-CS2 and PLA-CS3). The under face of the surfaces and the double-sided adhesive tape placed on each plate well were exposed to ultraviolet (UV) sterilization for 1 h. Then, the sterile surfaces were fixed at the bottom of each well and the plate was sterilized by UV radiation for more 1 h. After that, the wells were filled with 3 mL of *S. aureus*, *P. aeruginosa* or mixed bacterial suspensions previously prepared. The negative control was assessed by adding 3 mL of LB medium to the UV-sterilized surfaces to control their sterility through the experiments. The microplates were then incubated at 37 ˚C, for 24 h under static conditions to mimic the conditions typically found in some IMDs. All experiments were performed in three independent assays, each one with three replicas of each surface.

3.2.4.2. Cell supernatant analysis

After 24 h of biofilm formation on PLA, PLA-β-CS, PLA-CS1, PLA-CS2 and PLA-CS3 surfaces, the cell culture supernatants were analyzed to evaluate the antimicrobial effect of the synthesized CS surfaces against planktonic cells. For that, 100 µL of the supernatant of each well were collected and used to perform serial dilutions in NaCl solution (8.5 $g.L^{-1}$), which were spread on PCA (Merck KGaA, Germany) plates and incubated overnight at 37 ˚C. PCA supplemented with tetracycline was used to select mCherry-*P. aeruginosa* colonies. After incubation, the number of CFU was determined ($CFU.mL^{-1}$).

3.2.4.3. Biofilm analysis

PLA and CS surfaces were detached from the microplate wells and transferred to 15 mL sterile Falcon tubes with 2 mL of 8.5 $g.L^{-1}$ NaCl solution. Falcon tubes were vortexed (ZX4, Velp Scientifica) for 3 min at full power, 3000 rpm [62], to obtain biofilm cell suspensions that were further analyzed using two different methodologies: CFU counting method to determine the number of culturable cells and epifluorescence microscopy using the Live/Dead kit to quantify the total and viable cells. The number of VBNC cells was determined by the difference between the number of viable and culturable cells [63]. The final values of total, viable, culturable and VBNC cells are presented as percentages of biofilm cells compared to the PLA surfaces (control). These percentages were estimated by the following Equation (1):

$$\text{Biofilm cells } (\%) = (\text{Cells}_{\text{CS-surface}} / \text{ Cells}_{\text{Control}}) \times 100 \quad (1)$$

where $\text{Cells}_{\text{CS-surface}}$ corresponds to the number of biofilm cells on the CS-based surfaces (in $cells.cm^{-2}$ or $CFU.cm^{-2}$) and $\text{Cells}_{\text{Control}}$ to the number of biofilm cells on PLA surfaces.

3.2.4.3.1. Colony-forming unit counts

The CFU method allowed to assess biofilm cells culturability. Hence, 5-fold serial dilutions of the biofilm suspensions were prepared in NaCl solution and 10 µL were spread on PCA (Merck KGaA, Germany) plates which were incubated overnight at 37 ˚C. A tetracycline solution at 1.25 $g.L^{-1}$ was used to select mCherry-*P. aeruginosa* colonies. After that, the culturable cells were enumerated ($CFU.cm^{-2}$) and the percentages of biofilm cells were estimated as previously described (Equation 1).

3.2.4.3.2. Epifluorescence microscopy

The number of total cells and the biofilm cell viability was assessed by epifluorescence microscopy by staining the biofilm suspension with Live/Dead® (L/D) BacLight™ Bacterial Viability kit (Invitrogen Life Technologies, Alfagene, Portugal) and analyzing in epifluorescence microscopy.

This staining kit is based on a dual procedure using two dyes, SYTO®9 and propidium iodide (PI), which are fluorescent nucleic acid markers. SYTO®9 penetrates all cells (both intact cells and cells with a damaged membrane), staining the cells in green, while PI only penetrates cells with impaired membranes, allowing to determine the number of dead cells in red [64]. The sum of green (viable) and red (non viable) cells corresponds to the number of total cells.

The procedures adopted followed the methodology previously described by Gomes et al. [65]. Briefly, 800 μL of the biofilm cell suspensions were filtered through a Nucleopore, Track-Etch Membrane (Whatman Int., USA) black polycarbonate membrane (pore size 0.2 mm) under vacuum. The vacuum was removed, and 50 μL of PI and 250 μL of SYTO®9 were placed over the membrane for 7 min. The stained membrane was transferred to a microscopic slide and analyzed under an epifluorescence microscope (Leica DM LB2, Germany) with a 100 × objective. Since this microscope was connected to a Leica DFC300 FX camera, it was possible to obtain a minimum of fifteen images from different fields of view of each of the stained samples. Finally, these images were analyzed using the ImageJ software (version 1.52p, National Institutes of Health, EUA) to quantify the number of total and viable cells (cells.cm^{-2}).

3.2.4.3.3. Biofilm architecture by Confocal Laser Scanning Microscopy

To assess the architecture of both single- and dual-species biofilms of *S. aureus* and *P. aeruginosa* developed on PLA-CS surfaces, biofilms were observed by CLSM [66]. *P. aeruginosa* biofilm cells were contrasted from the mCherry fluorescence signal, while *S. aureus* cells were counterstained in green with 6 μM SYTO®9 (Thermo Fisher Scientific, USA), a general nucleic acid stain. After staining, *S. aureus*, *P. aeruginosa* and *S. aureus* + *P. aeruginosa* biofilms were observed using a 40 × water immersion objective lens in an inverted microscope Leica DMI6000-CS (Leica Microsystems, Germany), applying an excitation wavelength of 488 nm (argon laser) and 633 nm (helium-neon laser). To collect the SYTO®9 and mCherry emission fluorescence, the emitted fluorescence was recorded within the ranges of 500 to 580 nm and 640 to 730 nm, respectively. A minimum of five stacks of horizontal plane images (512 × 512 pixels, corresponding to 387.5 × 387.5 μm) with a *z*-step of 1 μm was obtained for each biofilm sample.

The blend mode of the "Easy 3D" tool of IMARIS 9.1 software (Bitplane, Zurich, Switzerland) was used to reconstruct the three-dimensional (3D) projections of biofilm structures, directly from the *xyz* image series obtained from the CLSM acquisitions. The biovolume (μm^3.μm^{-2}) and biofilm thickness (μm) were determined by using the COMSTAT2 plug associated with the ImageJ software [67].

3.2.5. Statistical analysis

All experiments were carried out in triplicate and descriptive statistics were used to calculate mean and standard deviation (SD) or error for the number of biofilm cells (total, viable, VBNC, and culturable cells), and biovolume and thickness of biofilms formed on all tested surfaces. The normality of the variables' distributions was analyzed with the Kolmogorov-Smirnov and Shapiro-Wilk tests, which showed that data were not normally distributed. Differences between the number of cells obtained for PLA and CS-based surfaces were evaluated using the nonparametric Mann-Whitney test. Moreover, quantitative parameters obtained from confocal microscopy were compared using a one-way analysis of variance through an ANOVA test. All statistical analysis used a 95% significance level, which means that differences were reported as statistically significant for p-values < 0.05. Data analysis was performed using the IBM SPSS Statistics version 24.0 for Windows (IBM SPSS, Inc., Chicago, IL, USA).

4. Results and discussion

4.1. Systematic review

Bearing in mind the aim of investigating the antimicrobial and anti-adhesive potential of CS, it was elaborated a systematic review using combinations of the following search terms: “chitosan”, “medical applications”, “antimicrobial”, “antibiofilm”, “biofilm”, and “adhesion”. After searching the four defined databases, a total of 366 studies were found and reduced to 291 studies after the removal of duplicates. Subsequently, 12 studies found by cross-referencing were added to the initial studies and a total of 303 studies were screened. During the screening of titles and abstracts, the inclusion criteria were considered, and 256 studies were excluded for not fulfilling them. The remaining 47 articles were assessed for eligibility. Then, all articles were read in full and the exclusion criteria were applied. Among these, 7 studies were excluded because they did not evaluate the anti-adhesive or antibiofilm activity of CS-based surfaces. Therefore, a total of 40 articles resulted from the PRISMA methodology and were included in the qualitative analysis (Figure 5).

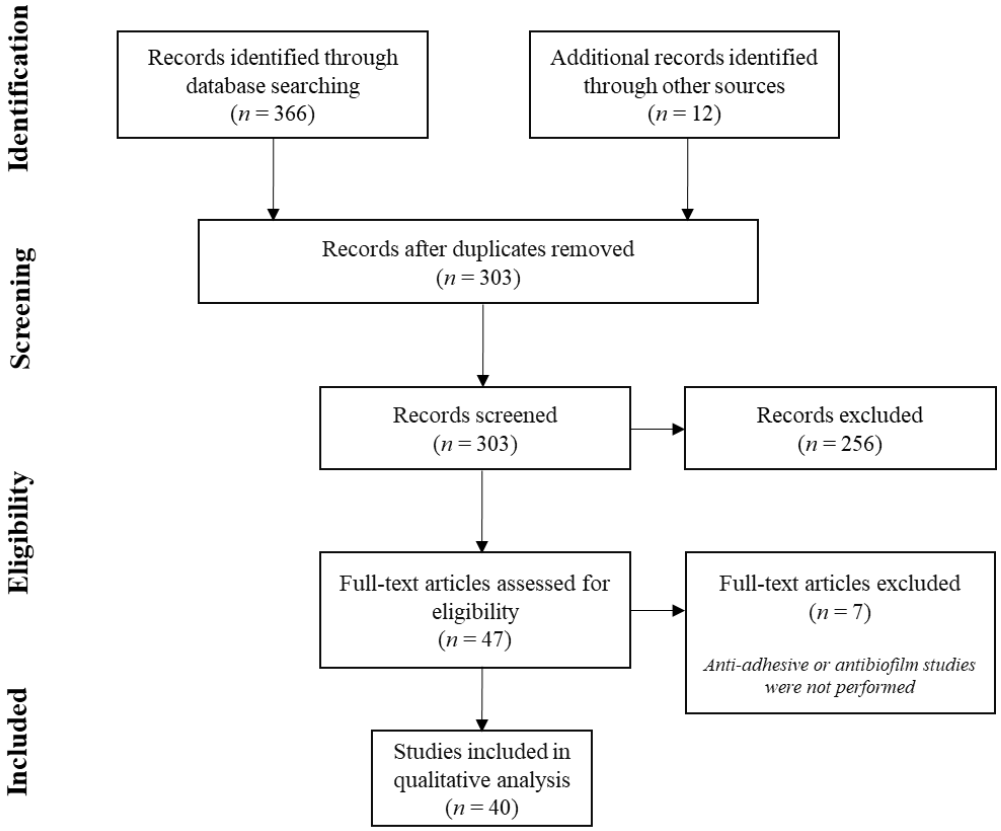


Figure 5. Summary of the literature search based on the PRISMA flow-chart.

The use of IMDs is a common and crucial medical procedure applied for both diagnosis and therapeutic purposes. However, the implantation of medical devices is frequently associated with the occurrence of difficult-to-treat infections due to microbial colonization and biofilm formation on their

abiotic surfaces [68]. The incidence of IAIs may be efficiently managed through the optimization of material surfaces. For this reason, in the last two decades, surface modification to provide antimicrobial properties to the materials and devices has been intensively investigated [69]. Despite the efforts to develop effective antimicrobial coatings, the majority of them may be toxic, trigger microbial resistance during prolonged use, and their clinical application is yet debatable [70-72].

Because of its high biocompatibility, biodegradability, and proven antimicrobial activity, chitosans have been introduced in the biomedical field to produce improved antimicrobial coatings for IMDs. In this systematic review, among the 40 articles referred to the anti-adhesive and antibiofilm activities of CS-based surfaces, 12 articles focused on exploring the potential of CS, and 7 studies evaluated the performance of functionalized chitosan (f-CS). The remaining 23 studies used CS in association with other compounds, among which 11 evaluated the efficacy of combining CS with antimicrobial compounds, 3 explored the potential of CS-metals association, 5 evaluated the conjugation of CS-polymers composites and 4 addressed the efficacy of CS conjugated with other compounds.

Figure B-1 in Appendix B summarizes the research progress on antimicrobial and anti-adhesive coatings based on CS alone or in association with other compounds with application in IMDs. The increasing number of studies in the last five years is considerable, especially for CS associated with antimicrobial compounds and functionalized CS.

Selected studies indicated that CS antimicrobial coatings were developed for application on a wide range of IMDs, including central venous catheters (17.5%), orthopedic implants (15.0%), and urinary catheters (12.5%). Moreover, most of the reviewed studies evaluated synthesized coatings against bacteria (82.5%) and only 10% of the studies were performed *in vivo*. This information suggests that a great part of antimicrobial and anti-adhesive CS coatings is yet far from a clinical application. On the other hand, about 30.0% of *in vitro* studies were performed under dynamic conditions, which may increase their predictive value [73].

When developing a new coating for biomedical applications, several features, including biocompatibility, hydrophilicity/hydrophobicity, antimicrobial activity and anti-adhesive properties, should be considered [74]. In this review, special attention was given to CS-based coatings with application in IMDs and their antimicrobial and anti-adhesive potential.

Chitosan-based coatings

Both *in vitro* and *in vivo* studies have demonstrated the potential of surfaces coated with CS to resist biofilm formation by bacteria and fungi. Table 1 summarizes the performance of CS antimicrobial coatings to inhibit microbial adhesion and biofilm formation on the surface of IMDs.

In 2010, Martinez et al. [75] demonstrated the antifungal and antibiofilm efficacy of CS against *Candida albicans* and *Candida parapsilosis* biofilms using a central venous catheter model. *In vitro* studies indicated that the viability of *Candida* spp. biofilms reduced 95% after 30 min of exposure, while *in vivo* studies demonstrated that the fungal burden on CS-coated catheters reduced 2.5-fold compared

to the untreated catheter. Also, SEM images revealed that biofilms formed on untreated surfaces were more extensive than on CS-coated catheters. The same authors also investigated the effect of CS on the inhibition of *in vitro* biofilm formation by *Cryptococcus neoformans* [76]. Results showed that the addition of exogenous CS to fungal biofilms significantly reduced yeast viability and metabolic activity, and prevented cell adhesion on polystyrene surfaces after 30 min of exposure, which is consistent with CS fungicidal activity [77]. In 2014, Pu et al. [78] also found that CS was able to reduce the metabolic activity and the viability of *C. albicans* biofilms in the early and intermediate phases of its development. This effect is the consequence of the physical stress imposed by CS on the fungal biofilm structures due to the permeabilization of cellular membranes, which allows penetration of CS molecules and its binding to DNA with subsequent inhibition of mRNA synthesis [79]. It is also likely that the interaction between positively charged CS molecules and negatively charged microbial cell membranes leads to the leakage of intracellular constituents, causing cell death [80]. Moreover, a net positive charge on the fungal surfaces may retain yeast cells in suspension, preventing biofilm formation [81]. Therefore, these findings suggest that CS is a promising alternative to current antifungal agents and can be used for designing antimicrobial coatings to protect medical device surfaces from fungal biofilm formation [75, 76, 78].

Likewise, the antimicrobial properties of CS-based coatings have also been demonstrated against a broad spectrum of Gram-positive and Gram-negative bacteria. A study developed by Bulwan et al. [82] revealed that CS-coated silicone films were effective in suppressing *S. aureus* biofilm formation and reducing the metabolic activity of adhered cells by 60% compared to uncoated films. The surface physical characterization indicated that the immobilization of CS molecules decreased the hydrophobicity and roughness of the synthesized films, making bacterial adhesion unfavourable [82]. Similarly, CS-coated polyurethane (PU) films reduced the number of *P. aeruginosa* and *S. aureus* adhered cells by 2-5 Log [69]. The authors concluded that CS immobilization improved surface hydrophilicity by increasing the number of polar groups, and thus, the bacterial adhesion decreased. In addition, these films reduced *P. aeruginosa* and *S. aureus* biofilm viability to 24.0 and 51.7%, respectively. As with fungal cells, the antibacterial action of CS results from the interaction between positively charged CS molecules and negatively charged cell membranes, which may prevent mass transfer across the cell wall and may lead to leakage of intracellular content [83]. Results also suggested that the antibacterial activity of CS-coated PU films was higher for *P. aeruginosa* than *S. aureus*, which may be explained by bacteria surface polarity. The outer membrane of Gram-negative bacteria is essentially composed of lipopolysaccharides containing phosphate and pyrophosphate groups which increase the negative charge density on the bacterial surfaces, leading to higher attraction to the positive CS surfaces compared to *S. aureus* cells [69]. Since then, the potential of CS surfaces to inhibit biofilm formation by Gram-negative bacteria has been vastly explored. In 2017, Costa et al. [84] also demonstrated that polystyrene films coated with CS reduced the biomass and metabolic activity of adhered *Acinetobacter baumannii* cells and biofilms by 93 and 43%, and 80 and 39%, respectively. Campana et al. [85] showed that segments of Foley urinary catheters coated with either high or low MW

CS were able to reduce *in vitro* bacterial adhesion by 70 and 58%, respectively, and only 20% of viable *Klebsiella pneumoniae* and *E. coli* cells were recovered from CS-treated catheters. In 2018, the same research group evaluated the potential of CS-coated urinary catheters to inhibit bacterial biofilm formation. Results revealed that coated catheters reduced *K. pneumoniae* and *E. coli* biofilm formation up to 6.3 Log [21]. The potential of CS molecules to inhibit *K. pneumoniae* biofilm formation (86.5% reduction) had previously been demonstrated [86].

Recently, Rubini et al. [87] studied the performance of CS-coated silicone catheters to inhibit *C. albicans, S. epidermidis* and mixed biofilms. Data demonstrated that CS-coated urinary catheters inhibited biofilm formation by 60-68%, depending on the biofilm development stage [87].

Although both low and high MW chitosans have displayed high efficacy to reduce microbial adhesion and biofilm formation on the surfaces of IMDs, some authors focused their attention on the study of low MW CS. Firstly, Cobrado et al. [88] showed that PU catheter segments coated with low MW CS decreased the metabolic activity of *S. epidermidis* and *C. albicans* biofilms by 80.5 and 87.5%, respectively after 24 h. Given these promising results, the authors also tested the efficacy of CS-coated PU catheters to inhibit *in vivo* biofilm formation [89]. The metabolic activity and biomass of *S. epidermidis* biofilms decreased by 57.6 and 41.3%, respectively, while *C. albicans* biofilms reduced their metabolic activity and biomass by 43.5 and 23.2%, respectively [89]. Comparing both studies, results indicated that the performance of CS-coated catheters decreased when tested *in vivo*, revealing the importance of testing antimicrobial coatings under conditions that mimic the clinic scenarios (either *in vivo* tests or experimental conditions closer to reality, e.g., controlled hydrodynamic conditions, temperature and culture medium).

In general, CS-based surfaces were able to decrease the fungal biofilm formation up to 65% and reduced the viability of biofilm cells by 95%, reduce the adhesion and biofilm formation of Gram-negative bacteria by 87 and 70%, respectively, and decrease the viability and metabolic activity of Gram-positive biofilms by 50 and 80%, respectively.

These data show the potential of chitosans to reduce not only the adhesion of human pathogens on medical devices, including urinary and central venous catheters, but also to prevent their re-growth ability.

Functionalized CS-based coatings

Numerous strategies have been explored to inhibit microbial adhesion and subsequent biofilm formation. Table 1 describes different CS functionalizations and their effect on the antimicrobial activity of CS-based coatings.

Several authors believe that the functionalization of CS molecules by the substitution of the -OH groups with $-CH_2COOH$, generating carboxymethyl chitosans (CM-CS) may enhance their intrinsic antimicrobial properties. In 2012, Wang et al. [90] produced silicone films pre-treated with polydopamine and impregnated with CM-CS and evaluated their efficacy to inhibit *E. coli* and *Proteus*

mirabilis adhesion and biofilm formation. These films reduced bacterial adhesion by more than 90% after 4 h and were effective in inhibiting biofilm formation under both static and flow conditions [90].

As IAIs are frequently caused by *Candida* spp., Tan et al. [91] evaluated the performance of silicone films coated with CM-CS against biofilms formed by single- and multi-*Candida* species. Although some studies have shown that mixed biofilms exhibit enhanced resistance compared with single-species biofilms, these authors indicated that both single and multi-species biofilms were inhibited by 70%. According to them, CM-CS may interrupt the interactions between different *Candida* species, inhibiting mixed biofilm formation [91]. Additionally, the CM-CS-coated silicone films were to be able to inhibit biofilm formation by multi-fungal and -bacterial species [91-93]. After 90 min, CM-CS films inhibited *S. epidermidis* and *C. albicans* adhesion by more than 90% [93]. Moreover, CM-CS films not only efficiently inhibited fungi and bacteria adhesion (> 90%) but also decreased mixed biofilm formation (70%) and its metabolic activity (60%) [92]. These effects may result from the intra- and intermolecular interactions between -COOH and $-NH_2$ groups, which lead to an increase in the number of $-NH_3^+$ groups [94]. Thus, the increased positive charges in CS molecules may potentiate their interaction with negatively charged cell membranes, improving their antimicrobial activity.

Also, the functionalization of CS with hydroxypropyltrimethyl ammonium chloride (HACC) increased its water solubility, antimicrobial activity, and biocompatibility, depending on the degree of substitution of the quaternary ammonium [95]. The effect of polymethylmethacrylate (PMMA) incorporated with HACC was evaluated on the inhibition of methicillin-resistant *S. aureus* (MRSA) and *S. epidermidis* biofilms. Data indicated that coated PMMA films significantly reduced biofilm viability through the inhibition of *icaAD* transcription that results in the downregulation of the production of polysaccharide intercellular adhesins [96].

Lastly, a recent study conducted by Niemczyk et al. [97] demonstrated that CS-fatty acid derivatives (an amphiphilic chitosan derivate) films reduced *E. coli* colonization by more than 80%. Based on previous results, the authors believe that CS-fatty acid derivatives are non-nutritive and can inhibit bacterial migration and growth [97].

Overall, these results suggest that the modifications introduced on the surface of CS molecules change their physicochemical properties, increasing the potential of CS coatings to reduce microbial adhesion and biofilm formation (by 90 and 70%, respectively).

Table 1. Studies reporting the anti-adhesive and/or antibiofilm efficacy of chitosan and functionalized chitosan.

Coating	Material	Medical application	Species	Major conclusions	Ref.
Chitosan	Polyethylene catheters [a,b]	Central venous catheters and other medical devices	*C. albicans* [1] *C. parapsilosis* [1]	*In vivo* studies: The fungal burden on CS-treated catheters reduced 2.5-fold compared to untreated catheters. SEM images demonstrated that biofilms formed on untreated catheters were more extensive than on CS catheters. *In vitro* studies: The viability of *Candida* sp. biofilms reduced 95% after 30 min.	[75]
	Polystyrene microtiter plates [b]	Indwelling medical devices	*C. neoformans* [2]	*C. neoformans* biofilms formed in the presence of 0.312 mg.mL^{-1} CS reduced their metabolic activity by 80%. Mature biofilms also significantly decreased their metabolic activity and viability ($p < 0.001$) after 30 min.	[76]
	Silicone [b]	Implantable devices or biosensors	*S. aureus* [3]	Results demonstrated that *S. aureus* biofilm formation was suppressed on CS-coated silicone films. In addition, biofilm metabolic activity on CS films reduced 60% compared to the uncoated films.	[82]
	n.d. [b]	Indwelling medical devices	*K. pneumoniae* [4]	Chitosan (0.0625 mg.mL^{-1}) induced a biofilm reduction of 86.5%.	[86]
	Glass [b]	Indwelling medical devices	*C. albicans* [1]	Results demonstrated that 0.0313% CS killed more than 50% of cells in the early and intermediate phases of biofilm development.	[78]
	Polyurethane films [b]	Indwelling medical devices	*P. aeruginosa* [5] *S. aureus* [3]	Chitosan (0.5%)-coated films reduced *P. aeruginosa* and *S. aureus* biofilm viability by 24.0 and 51.7 %, respectively.	[69]
	Polystyrene films [b]	Indwelling medical devices	*A. baumannii* [6]	*A. baumannii* adhered to CS-coated films showed a reduction of biomass and metabolic activity of 93 and 43%; biofilm biomass and metabolic activity were also inhibited by 80 and 39%, respectively.	[84]
	Foley urinary catheter segments [b]	Urinary catheters	*E. coli* [7] *K. pneumoniae* [4]	High and low MW CS reduced bacterial adhesion by 70 and 58%, respectively. A low percentage of viable *K. pneumoniae* and *E. coli* cells (about 20%) were recovered from catheters after CS treatments.	[85]
	Foley urinary catheter segments [b]	Urinary catheters	*E. coli* [7] *K. pneumoniae* [4]	After 48 h, CS-coated catheters were able to reduce *K. pneumoniae* and *E. coli* biofilm formation up to 6.3 Log.	[21]
	Silicone catheters segments [b]	Urinary catheters	*C. albicans* [1] *S. epidermidis* [3]	CS-coated catheters inhibited *C. albicans*, *S. epidermis* and mixed biofilms by 68, 65 and 60%, depending on their development stage.	[87]
Low molecular weight CS	Polyurethane-like catheters segments [b]	Central venous catheters	*A. baumannii* [6] *C. albicans* [1] *S. epidermidis* [3] *S. aureus* [3]	Chitosan (78 mg.mL^{-1}) reduced the biofilm metabolic activity of *S. epidermidis* by 80.5%, CS (5.0×10^3 mg.mL^{-1}) reduced the *C. albicans* biofilm metabolic activity by 87.5 and 90.0% after 24 and 48 h, respectively.	[88]

n.d., not described; [a], *in vivo* study; [b], *in vitro* study; [*], study performed under hydrodynamic conditions.
[1] *Candida* sp.; [2] *Cryptococcus* sp.; [3] *Staphylococcus* sp.; [4] *Klebsiella* sp.; [5] *Pseudomonas* sp.; [6] *Acinetobacter* sp.; [7] *Escherichia* sp.; [8] *Proteus* sp.; [9] *Lactobacillus* sp.; [10] *Rothia* sp.; [11] *Streptococcus* sp. MRSA, methicillin-resistant *Staphylococcus aureus*.

Table 1. (continued).

Coating	Material	Medical application	Species	Major conclusions	Ref.
Low molecular weight CS	Polyurethane catheter segments [a]	Central venous catheters	*A. baumannii* [6] *C. albicans* [1] *S. epidermidis* [3] *S. aureus* [3]	The metabolic activity and total biomass of *S. epidermidis* biofilms decreased by 57.6 and 41.3%, respectively, in CS-catheters (80 $mg.mL^{-1}$ CS). In turn, *C. albicans* biofilms reduced their metabolic activity and biomass by 43.5 and 23.2%, respectively, in treated catheters (2.5×10^{3} $mg.mL^{-1}$).	[89]
Functionalized-CS					
Carboxymethyl chitosan	Silicone pre-treated with polydopamine [b,*]	Medical devices	*E. coli* [7] *P. mirabilis* [8]	Carboxymethyl CS coating reduced the *E. coli* and *P. mirabilis* adhesion by more than 90% after 4 h. Biofilm formation was also inhibited on CS coating under static and flow conditions.	[90]
	Silicone films [b]	Indwelling medical devices	*C. tropicalis* [1] *C. parapsilosis* [1] *C. krusei* [1] *C. glabrata* [1]	*Candida* spp. biofilm formation was inhibited by 70% for single species and 73.4% for multi-species biofilms.	[91]
	Medical-grade silicone [b,*]	Voice prosthesis	*C. albicans* [1] *C. tropicalis* [1] *L. gasseri* [9] *R. dentocariosa* [10] *S. epidermidis* [3] *S. salivarius* [11]	Carboxymethyl chitosan-coated films displayed a surface coverage of 4% less than untreated films.	[98]
	Medical-grade silicone [b]	Voice prosthesis	*C. albicans* [1] *C. tropicalis* [1] *L. gasseri* [9] *R. dentocariosa* [10] *S. epidermidis* [3] *S. salivarius* [11]	Carboxymethyl CS inhibited the adhesion of fungi and bacteria with an efficiency greater than 90%. CS coatings inhibited mixed biofilm formation by 73% and decreased their metabolic activity by more than 60%.	[92]
	Medical-grade silicone [b,*]	Indwelling medical devices	*C. tropicalis* [1] *S. epidermidis* [3]	After 90 min, more than 90% of cells were unable to adhere to carboxymethyl CS (2.5 $mg.mL^{-1}$)-coated surfaces. Coated silicone films also inhibited *S. epidermidis*, *C. tropicalis* and mixed biofilm formation by 64.1, 66.6 and 54.7%, respectively.	[93]
Fatty acid derivatives	Poly(ethylene terephthalate) and butylene dilinoleate (50:50) polymer [b]	Catheters	*E. coli* [4]	*E. coli* colonization on CS/fatty acid derivatives coatings was reduced by more than 80%.	[97]
Quaternised chitosan derivative	Polymethyl-methacrylate (PMMA)-based cement [b,*]	Orthopedic implants	MRSA [3] *S. epidermidis* [3]	The viability of biofilms formed on functionalized-CS-PMMA surfaces was significantly lower than on PMMA surfaces ($p < 0.01$).	[96]

n.d., not described; [a], *in vivo* study; [b], *in vitro* study; [*], study performed under hydrodynamic conditions.
[1] *Candida* sp.; [2] *Cryptococcus* sp.; [3] *Staphylococcus* sp.; [4] *Klebsiella* sp.; [5] *Pseudomonas* sp.; [6] *Acinetobacter* sp.; [7] *Escherichia* sp.; [8] *Proteus* sp.; [9] *Lactobacillus* sp.; [10] *Rothia* sp.; [11] *Streptococcus* sp. MRSA, methicillin-resistant *Staphylococcus aureus.*

Coatings based in CS associated with antimicrobial compounds

As some authors have reported that CS had no antimicrobial activity at pH 7.0 due to the deprotonation of amino groups and its poor solubility in water [94], extensive research has been carried out to improve the CS antimicrobial action and extend its use in a broader pH range through the incorporation of antimicrobial agents or peptides into the CS materials [99]. Table 2 lists studies reporting the efficacy of CS and antimicrobial compound conjugates.

An ideal antimicrobial coating should not only exhibit an initial anti-adhesive ability but also display a long-term prophylactic and antimicrobial performance. In the last years, the association of CS with antimicrobial agents has been explored as an alternative to improve the efficacy of available drugs due to their synergic mechanisms of action and the chitosans' ability to control the release of active agents [100].

In this context, Cao and Sun [101] developed a rifampicin-CS coating for long-term medical devices based on a system that produces localized concentrations of antibiotics on material surfaces using a cationic surfactant. Synthetized films avoided *Staphylococcus* spp. adhesion even after 72 h incubation. This excellent antimicrobial durability is associated with the formation of a stable complex between the CS and anionic antibiotics and its controlled diffusion mechanism [101]. In 2018, Zhou et al. [102] immobilized tobramycin-loaded micelles embedded in CS/heparin polydopamine on titanium surfaces. The number of adhered bacteria was significantly lower on tobramycin-CS/heparin polydopamine coatings compared to the control ($p < 0.05$). These results indicated that synthesized coatings were capable of long-term tobramycin release in acid environments (pH 4.3), probably because the protonated amino group of CS strengthens the electrostatic interaction with micelles keeping them intact and stable [102]. Thus, antibiotic-loaded micelles displayed pH-sensitive capability and high-loading efficiency, exhibiting a "long-term release" pattern which is desirable for preventing postoperative infections associated with orthopedic implants insertion [102].

Also, Ajdnik et al. [100] coated CS nanoparticles with amoxicillin/clavulanic acid and deposited them onto silicone material. Silicone films coated with amoxicillin/clavulanic acid exhibited a high efficacy (> 93%) in the prevention of *S. aureus* biofilm formation up to 1 month of exposure. Therefore, this result indicates the high efficacy of this coating to prevent biofilm formation on tympanostomy tubes [100]. Lastly, Valverde et al. [103] synthesized a new coating containing hyaluronic acid-chitosan polyelectrolyte multilayers deposited on modified titanium surfaces for application in medical implants. Subsequently, produced coatings were loaded with triclosan, a disinfectant agent with proven efficacy. Results demonstrated that *S. aureus* cells adhered to hyaluronic acid-CS surfaces lost their viability by 72%, while bacteria attached to the hyaluronic acid-CS/triclosan-coated surfaces completely lost their viability. Multilayers were able to release triclosan within the initial period of bacterial adhesion through the degradation of the outer layers, which are more weakly attached, especially in the first 10 h [103].

Altogether these studies revealed the potential of CS to control the release of active antimicrobial agents on the IMD surfaces with different indwelling times.

Natural defense substances secreted by living organisms have emerged as an attractive class of biocidal agents. Numerous natural enzymes exhibit antimicrobial or antibiofilm abilities with different functions, such as killing microbes by direct contact, interfering with biofilm formation, disrupting the biofilm matrix, inhibiting QS or catalyzing reactions to produce antimicrobial compounds [104].

Table 2. Studies reporting the efficacy of coatings based on chitosan associated with antimicrobial compounds.

CS-based coatings	Material	Medical application	Species	Major conclusions	Ref.
Antimicrobial agents					
Rifampicin	CS films [b,*]	Long-term medical devices	*S. aureus* [1] *S. epidermidis* [1]	Bacterial cells were not able to grow on CS-rifampicin surfaces after 72 h incubation.	[101]
pH-responsive tobramycin-embedded micelles	Polydopamine-modified titanium surfaces [b]	Orthopedic implants	*E. coli* [2] *S. aureus* [1]	Adhered bacteria were significantly lower (p <0.05) on CS-tobramycin-coated surfaces than on the control group at 4 (1.18%), 12 (0.16%), 24 (0.25%), 48 h (0.23%).	[102]
Amoxicillin/clavulanic acid (CoAM)	Silicone [b,*]	Tympanostomy tubes	*S. aureus* [1]	CS-CoAM-coated silicone films exhibited a high efficacy (> 93%) in the prevention of biofilm formation on the tube surface.	[100]
Disinfectant agents					
Hyaloronic acid (HA)/triclosan	Modified titanium surfaces [b,*]	Medical implants	*S. aureus* [1]	Bacteria adhered to CS-HA surfaces lost their viability by 72%, while bacteria attached to the CS-HA/triclosan-coated surface showed a total loss in viability.	[103]
Enzymes					
Lysozyme	Stainless steel surfaces [b]	Medical implants and devices	*S. aureus* [1]	*S. aureus* viability decreased by more than 70% after 2 h incubation with CS-lysozyme coatings, and > 95% after 4 h.	[99]
Proteases	n.d. [b]	Indwelling medical devices	*L. monocytogenes* [3] *P. aeruginosa* [4] *S. aureus* [1]	The antibiofilm activity of proteases was observed after 24 h of incubation; bead mobility was increased with Protease B (36%), Alcalase (57%) and Neutrase (84%).	[105]
Cellobiose dehydrogenase (CDH) and deoxyribonuclease I (DNase)	Polystyrene microtiter plates [b]	Indwelling medical devices	*C. albicans* [5] *S. aureus* [1]	Biofilms of *S. aureus*, *C. albicans* or mixed species were inhibited by CS nanoparticles-DNase-CDH by 99, 89 and 91%, respectively. In addition, these composites caused 80% biofilm disruption on mono- and polymicrobial biofilms.	[104]

n.d., not described; [a], *in vivo* study; [b], *in vitro* study; [*], study performed under hydrodynamic conditions.
[1] *Staphylococcus* sp.; [2] *Escherichia* sp.; [3] *Listeria* sp.; [4] *Pseudomonas* sp.; [5] *Candida* sp.

Table 2. (continued).

CS-based coatings	Material	Medical application	Species	Major conclusions	Ref.
Antimicrobial peptides (AMP)					
Hyaluronic acid (HA)/β-peptide (coumarin-linker-(ACHC-B3hVal-B3hLys)3	Polyethylene catheters [a,b]	Central venous catheters	*C. albicans* [5]	*In vitro* studies: Biofilms formed on CS-HA-coated catheters reduced their metabolic activity by 80% compared to control. Catheter loading with β-peptide resulted in substantial reductions in biofilm growth (≈10%). *In vivo* studies: Biofilms formed on CS-HA-coated catheters were less robust than those observed on bare catheters. Tubes coated with β-peptide-loaded CS-HA films exhibited either no or very few yeast cells.	[106]
	Titanium surfaces [b]	Orthopedic implants	*S. aureus* [1]	Results demonstrated that coatings loaded with β-peptide prevented the formation of *S. aureus* biofilms for up to 24 days. After 36 days, biofilm viability reduced 60% compared to bare titanium.	[107]
α-helical AMP MSI-78(4-20) (KFLKKAKKFGKAFVKIL)	Gold substrates [b]	Bone implants and other medical devices	*S. epidermidis* [1]	The AMP-chitosan coating did not significantly reduce bacterial adhesion but decreased the viability of adhered cells by 60%.	[108]

n.d., not described; [a], *in vivo* study; [b], *in vitro* study; [*], study performed under hydrodynamic conditions.
[1] *Staphylococcus* sp.; [2] *Escherichia* sp.; [3] *Listeria* sp.; [4] *Pseudomonas* sp.; [5] *Candida* sp.

In 2013, Yuan et al. [99] covalently immobilized CS with glutaraldehyde on stainless steel surfaces and conjugated lysozyme on grafted CS to enhance its biocidal effect to inhibit *S. aureus* adhesion and biofilm formation on medical implants and devices. Bacterial viability decreased by more than 70% after 2 h and more than 95% after 4 h of exposure. Results demonstrated that the antibacterial activity of CS may combine with that of the immobilized lysozyme to give rise to a surface with high antibacterial activity, which effectively kills bacteria by contact even under neutral pH conditions [99]. It is known that lysozyme damages the cell wall of Gram-positive bacteria by catalyzing the hydrolysis of β (1,4) linkages between N-acetyl-muramic acid and N-acetyl-d-glucosamine residues of the peptidoglycan [109]. Additionally, several authors have previously reported that lysozyme covalently bound to polymeric films, silicone, and stainless steel exhibited good antimicrobial activity against bacteria [99].

Some biological disrupting enzymes have been used with success against bacterial biofilms. In a previous study, Elchinger et al. [110] reported that some proteases have activity against *S. aureus* and *S. epidermidis* biofilms. Based on these results, the authors immobilized these enzymes on CS surfaces to obtain films with improved antibiofilm activity [105]. The mobility of *Listeria monocytogenes*, *P. aeruginosa* and *S. aureus* increased with protease B (36%), alcalase (57%), and neutrase (84%) after 24 h incubation, at pH 7 and 37 °C [105]. Results indicated that these enzymes were effective in the early phases of biofilm development, probably due to their interaction with bacterial adhesins, which are early specific ligands to host factors [111]. Recently, Tan el al. [104] co-immobilized cellobiose

dehydrogenase (CDH) and deoxyribonuclease I (DNase) on CS nanoparticles and tested its antibiofilm activity against *C. albicans* and *S. aureus* mono- and polymicrobial biofilms. CS-DNase-CDH nanoparticles inhibited *S. aureus, C. albicans,* and mixed biofilms by 99, 89 and 91%, respectively. Additionally, these nanoparticles caused 80% biofilm disruption on mono- and polymicrobial biofilms. These exceptional results were attributed to the triple-action of CS, DNase and CDH. Firstly, CS not only exerts its antimicrobial activity but also improves the stability and usability of co-immobilized enzymes. Secondly, it is known that DNase can disrupt biofilm matrix and enhance its antimicrobial activity when combined with antimicrobial compounds. Thirdly, CDH generates hydrogen peroxide which possesses the ability to inhibit microbial growth and biofilm formation [104].

Another way to improve CS antimicrobial activity consists of the incorporation of antimicrobial peptides (AMPs) into the CS materials. AMPs have been studied as potential new classes of antimicrobial agents. Their mechanism of action involves the disruption of the microbial cell membranes, leading to membrane permeabilization, cell lysis and subsequent cell death [112]. Moreover, due to the lack of a single target, the development of microbial resistance to AMPs and their mimetics may be lower than for traditional antimicrobial agents [113].

In 2016, Raman et al. [106] designed a polyelectrolyte multilayer coating (CS and hyaluronic acid) that had inherent antifungal properties as a platform for the immobilization and surface-mediated release of antimicrobial peptides (β-peptide) and tested its *in vitro* and *in vivo* efficacy to inhibit biofilm formation on central venous catheters. *In vitro* studies demonstrated that hyaluronic acid-CS-coated catheters loaded with β-peptide improved the efficacy of hyaluronic acid-CS catheters by 10%. Likewise, in *in vivo* studies, treated catheters loaded with β-peptide exhibited either none or very few yeast cells. These results suggested that the controlled intraluminal release of β-peptide resulted in a substantial reduction of biofilm growth [106].

As β-peptides also demonstrated strong antibacterial activity against Gram-positive and Gram-negative bacteria, Lopez et al. [107] evaluated the coating system described above on titanium surfaces to inhibit *S. aureus* biofilm formation. Results indicated that coatings loading with β-peptide prevented *S. aureus* biofilms formation for up to 24 days. After 36 days, biofilm viability reduced 60% compared to titanium surfaces [107].

Recently, Monteiro et al. [108] covalently bonded α-helical AMP (KFLKKAKKFGKAFVKIL) to a CS coating and tested its performance to prevent *S. epidermidis* adhesion on bone implants and other medical devices. The AMP-chitosan coating did not significantly reduce bacterial adhesion but decreased the cell viability of adhered cells by 60% [108].

The immobilization of AMPs on CS surfaces provides good surface availability and homogenous distribution of the AMP on the surface while reducing enzymatic degradation and thus increasing its long-term stability.

Among described strategies, enzymes and antimicrobial peptides have shown promising results in the development of broad-spectrum antimicrobial surfaces for IMDs.

Coating based on CS associated with metals

Several studies have reported the synergic association between CS and silver or other metals to prevent biofilm-related infections. Table 3 lists the studies reporting the efficacy of CS conjugated with metals.

The broad and strong antibacterial activity of silver is already well known. Wang et al. [114] produced silver nanoparticles (AgNPs) doped CS/polyvinylpyrrolidone (PVP) films to reduced *E. coli* and *S. aureus* adhesion on IMDs. In fact, AgNPs-CS/PVP composites were able to reduce bacterial adhesion up to 100% [114].

Yang et al. [115] incorporated AgNPs into catechol (a natural antibiotic)-CS coatings by adding silver nitrate solutions using the conjugated catechol groups as reducing agents and evaluated the effectiveness of these coatings to inhibit bacterial adhesion on polyurethane films. During initial adhesion, the number of live *E. coli* cells decreased 44% in catechol-CS/AgNPs-coated films compared to catechol-CS-coated films [115], confirming the antibacterial activity of silver nanoparticles.

Table 3. Studies reporting the efficacy of coatings based on chitosan associated with metals.

CS-based coatings	Material	Medical application	Species	Major conclusions	Ref.
Silver nanoparticles (AgNPs)/polyvinylpyrrolidone (PVP)	Silicone wafers and polyethylene sheets [b,*]	Medical devices	*E. coli* [1] *S. aureus* [2]	Chitosan-AgNPs/PVP composites displayed higher antimicrobial activity than polyethylene films (inhibition zone 4 mm vs. 0 mm, respectively). In addition, these films reduced *S. aureus* and *E. coli* adhesion up to 100%.	[114]
Zinc oxide/polyaniline (ZnO/PANI) composite	Glass [b]	Indwelling medical devices	*C. albicans* [3] *P. aeruginosa* [4] *S. aureus* [2]	CS-ZnO/PANI coatings inhibited *S. aureus* and *P. aeruginosa* biofilm formation by more than 95%. The antimicrobial activity of CS–ZnO/PANI composite against established biofilms resulted in more than 95% inhibition.	[116]
Iron oxide nanoparticles	Polystyrene microtiter plates [b]	Orthopedic implants	*S. aureus* [2]	CS-coated iron oxide nanoparticles decreased the number of biofilm cells up to 3 Log and its metabolic activity by 50% compared to the control.	[117]
Catechol/Silver nanoparticles	Polyurethane films [b,*]	Urethral catheters	*E. coli* [1] *S. aureus* [2]	During the initial adhesion, live *E. coli* cells significantly decreased in the CS-catechol hydrogel-coated films, and further decreased in the CS-catechol/AgNPs-coated films compared to the bare substrate (bare: 85.23%, CS-catechol hydrogel coating: 48.32%, CS-catechol hydrogel coating with AgNPs: 4.70%).	[115]

[a], *in vivo* study; [b], *in vitro* study; [*], study performed under hydrodynamic conditions.
[1] *Escherichia* sp.; [2] *Staphylococcus* sp.; [3] *Candida* sp.; [4] *Pseudomonas* sp.

Similar to silver, the majority of inorganic materials possess superior durability and selectivity and can produce high levels of reactive oxygen species, enhancing microbial cell damages. Among the several types of metals, zinc oxide nanoparticles (ZnONPs) display antibacterial and antifungal activities at low concentrations [118]. The immobilization of ZnONPs on CS-polyaniline composites inhibited *S. aureus* and *P. aeruginosa* biofilm formation and pre-established biofilms by more than 95% [116].

Iron oxide nanoparticles have also been studied in recent years, demonstrating good antibacterial activity. Shi et al. [117] developed CS-coated iron oxide nanoparticles to prevent biofilm formation by *S. aureus* in orthopedic implants. The produced coatings decreased the number of biofilm cells up to 3 Log and biofilm metabolic activity by 50% [117].

In general, the CS association with metals to generate antimicrobial coatings effectively reduced fungal and bacterial adhesion (> 95%) on medical surfaces.

Coatings based on CS associated with polymers

It is known that the properties of medical surfaces, including hydrophobicity or hydrophilicity, and the presence of surface charges have a high impact on initial microbial adhesion and proliferation [119]. For this reason, several studies have proposed surface modification with CS and polymers conjugates to inhibit or modulate microbial colonization. Table 4 describes the efficacy of antimicrobial coatings based on CS associated with polymers.

In 2013, Silva-Dias et al. [120] investigated the *in vitro* and *in vivo* antibiofilm activity of low MW CS hydrogel to prevent *Candida* spp. biofilm formation on central venous catheters. Catheter segments coated with CS hydrogel significantly reduced the metabolic activity (95.7%) of *C. parapsilosis* biofilms formed *in vivo*. Coatings composed of poly(lactic-co-glycolic) acid (PLGA) and CS were also able to decrease by 2-fold the viability of *S. aureus* biofilms compared to uncoated surfaces [121]. In fact, PLGA is a relatively hydrophobic polymer that might be used as a scaffold in association with CS, increasing its bioactivity, bioavailability and biocompatibility [121]. Lastly, the association of hyaluronic acid and CS immobilized on polyethylene catheters or titanium surfaces displayed promising results [106, 112]. *In vitro and in vivo* studies demonstrated that catheters coated with hyaluronic acid-CS reduced the metabolic activity of *C. albicans* biofilms by 80% and the biofilms formed on these surfaces were less robust than those formed on bare catheters [106]. Also, *S. aureus* cells adhered to hyaluronic acid-CS surfaces lost their viability by 72% [103]. Hyaluronic acid is a natural polysaccharide that plays an important role in early- and long-range interactions between cells and substrates due to its hydrophilic nature [103].

In general, the association of CS with polymers resulted in improved antimicrobial and anti-adhesive coatings with desirable properties (e.g., biocompatibility and durability) for medical implants.

Table 4. Studies reporting the efficacy of coatings based on chitosan associated with polymers.

CS-based coatings	Material	Medical application	Species	Major conclusions	Ref.
Low molecular weight chitosan hydrogel	Polystyrene plates Polyurethane catheters [a,b]	Central venous catheters	*C. albicans* [1] *C. parapsilosis* [1] *C. glabrata* [1] *C. tropicalis* [1] *C. guilliermondii* [1]	*In vivo* studies: Catheter segments soaked with low MW CS-hydrogel significantly impaired the biofilm metabolic activity of *C. parapsilosis* (95.7 % ± 3.3). *In vitro* studies: The highest CS-tested concentration (1×10^4 mg.L^{-1}) caused the biofilm biomass and metabolic activity reductions of all *Candida* spp. up to 99% compared to non-treated biofilms.	[120]
Poly(lactic-co-glycolic) acid	n.d. [b]	Medical prosthetic devices	*S. aureus* [2]	Biofilms formed on CS-nanocoated surfaces contain at least 2-fold less viable cells compared to uncoated surfaces.	[121]
Hyaloronic acid (HA)	Polyethylene catheters [a,b]	Central venous catheters	*C. albicans* [1]	*In vitro* studies: Biofilms formed on CS-HA-coated catheters reduced their metabolic activity (80%) compared to control. *In vivo* studies: Biofilms formed on CS-HA-coated catheters were less robust than those observed on bare catheters.	[91]
	Modified titanium surfaces [b,*]	Medical implants	*S. aureus* [2]	Bacteria adhered to CS-HA surface lost their viability by 72%.	[103]

n.d., not described; [a], *in vivo* study; [b], *in vitro* study; [*], study performed under hydrodynamic conditions.
[1] *Candida* sp.; [2] *Staphylococcus* sp.

Coatings based on CS associated with other compounds

In this review, antimicrobial coatings based on CS associated with other compounds were also addressed as promising materials for the construction of IMDs.

In 2016, Visan et al. [122] blended CS to biomimetic apatite films, which were deposited by the combinatorial Matrix-Assisted Pulsed Laser Evaporation method on titanium discs and investigated their efficacy to prevent *E. coli* and *S. aureus* biofilm formation on bone implants. Apatite-CS surfaces reduced biofilms viability by 1 and 2 Log for *E. coli* and *S. aureus*, respectively, after 48 h of exposure [122]. Other authors produced silicone-based catheters coated with CS and alginate (an anionic polysaccharide) [123]. Data demonstrated that there were no *S. aureus* cells on alginate-CS coating, probably because of its anti-adhesive and antimicrobial activities [123]. In turn, Zhang et al. [124] immobilized heparin (an anticoagulant) and CS on titanium surfaces to avoid *E. coli* and *S. aureus* biofilm formation on blood-contact medical devices. Compared to titanium, the number of bacterial cells was significantly lower on heparin-CS coatings [124]. Yang et al. [115] developed catechol-modified CS coatings to inhibit bacterial adhesion on polyurethane films. During initial adhesion, the number of live *E. coli* cells decreased by 37% in catechol-CS-coated films compared to bare

polyurethane [115]. Under physiological or alkaline conditions, catechol groups transform into reactive o-quinones, which interact with many other functional groups acting as a natural antibiotic [115].

Although the described coatings revealed a promising antimicrobial activity, it is unknown if this activity is mainly due to the CS. Therefore, further research involving these compounds is required.

4.2. Experimental results

4.2.1. Characterization of synthesized surfaces

After synthesizing the surfaces by immobilization of CS and its derivatives in PLA films through the dip coating method, INL performed a characterization of PLA and CS-coated PLA surfaces since it is known that surface properties influence microbial adhesion and consequent biofilm formation [125, 126]. Hence, all surfaces were analyzed concerning the hydrophobicity (by the water contact angle measurement), the intermolecular interactions between CS and PLA (by FTIR analysis), and the morphology (by SEM analysis).

The hydrophobicity of the synthesized antimicrobial surfaces is a parameter that should be evaluated since it influences the adhesion of bacterial cells to the surface. Since the surface of bacterial cells has a hydrophobic nature, bacteria are more likely to attach to hydrophobic than hydrophilic biomaterials due to a reduction of the surface free energy [35, 127, 128]. The water contact angle values of PLA and CS-based surfaces are presented in Table C-1 in Appendix C, and their representative images are represented in Figure C-1 in the same appendix. Bearing in mind that the behavior of a surface is considered hydrophobic when the contact angle with water presents values higher than 90º [129], the analysis of the data obtained showed that both PLA and CS-coated PLA surfaces have hydrophilic characteristics. Furthermore, results demonstrated that the immobilization of CS and its derivatives onto PLA films decreased water contact angle values by an average of 30%. The increased hydrophilicity of the CS-coated surfaces can be justified by the increased number of polar groups compared to PLA films, proving the effectiveness of CS incorporation. Considering that previous studies reported that bacteria are more likely to adhere to hydrophobic surfaces [127, 128], coating PLA surfaces with CS may be a promising strategy to reduce bacterial adhesion and consequent biofilm formation on IMDs. It is also noteworthy that no dependency relationship was found between the MW of the CS used in the coating and the surface wettability. In fact, data showed that all CS-based surfaces tested (PLA-β-CS, PLA-CS1, PLA-CS2 and PLA-CS3) had a similar hydrophilic character since their water contact angle is close to 40º. This result is in agreement with a previous study that revealed that the wettability of CS functionalized surfaces is not affected by the MW of this polymer [130].

Since biomaterial surface topography can affect bacterial adhesion [6], INL also performed a Fourier Transform Infrared Spectroscopy (FTIR) and Scanning Electron Microscopy (SEM) analysis. FTIR enabled the evaluation of the chemical modifications of the CS-coated PLA surfaces compared with the uncoated PLA surfaces (Figure C-2 in Appendix C). It was verified that chemical interactions

between CS and PLA exists and CS was successfully immobilized on PLA film, since the presence of characteristic bands of CS was observed in the spectrum [130]. Furthermore, it was found that the CS MW did not influence its interaction with PLA, since the spectra of all the CS-based surfaces were similar. This result corroborates a previous study, which stated that there were no differences between the FTIR spectra of medium and low MW CS [131]. SEM analysis allowed to analyze the morphology of the surfaces and the distribution of the CS molecules into the PLA films. Representative images of the control (PLA) and of the surfaces functionalized with the higher and lower MW CS are represented in Figure C-3 in Appendix C. Contrary to the noticeable homogeneity observed on PLA surfaces, PLA surfaces coated with CS had small aggregates, whose formation may be associated with the presence of insoluble CS material. In fact, the poor solubility of this polymer has motivated extensive research to increase it and extend the use of CS to a broader range of environmental conditions [94]. Moreover, SEM analysis demonstrated that CS MW has an impact on surface morphology since the number of small aggregates decreased from the surface coated with the CS of highest MW (β-CS, MW= 294 kDa) to the surface with the lowest MW CS (CS3, MW= 61 kDa). In agreement with what was reported in a previous study developed by Peng et al. [95], the higher homogeneity in the dispersion of CS molecules observed on the PLA-CS3 surface can be explained by the increased solubility of CS in water when it is functionalized [95].

4.2.2. Cell supernatant analysis

The activity and stability of the immobilized chitosan (β-CS, CS1, CS2 and CS3) were monitored by incubating the surfaces with cell suspensions of *S. aureus* and *P. aeruginosa* (1×10^7 CFU.mL^{-1}) for 24 h. PLA film was used as control. Then, the number of culturable bacteria that remained in the supernatant was determined by CFU counting. The number of culturable cells of *S. aureus* and *P. aeruginosa* increased in a range of 1-36% and 21-74%, respectively, compared to PLA (Figure 6).

These results demonstrate significant differences between the supernatant composition on the control surfaces (PLA) and the CS-based surfaces, corroborating the presence of CS on functionalized PLA films. Moreover, considering the antimicrobial properties of CS described in the literature, if there was a release of the polymer from the coating, a reduction in the number of cells in the supernatant would be expected. However, it was observed that the CS-based surfaces did not reduce the number of culturable cells in the supernatant (Figure 6a-b), indicating that the polymer was effectively impregnated into the coating.

Furthermore, this analysis demonstrated that the immobilized CS significantly increased the concentration of both Gram-positive and Gram-negative bacteria in the supernatant compared to PLA films, which may be indicative of the anti-adhesive activity of CS-based surfaces. Assuming that the bacterial growth is similar in all wells, by mass balance, it is expected that the surfaces whose supernatant had a smaller amount of cells are those on which there was higher bacterial adhesion. Thus,

the increase up to 36 and 74% in the amount of *S. aureus* and *P. aeruginosa* cells, respectively, in the supernatant on the surfaces functionalized with CS may be indicative of the antibiofilm activity of this polymer (which will be discussed in the Section 4.2.3).

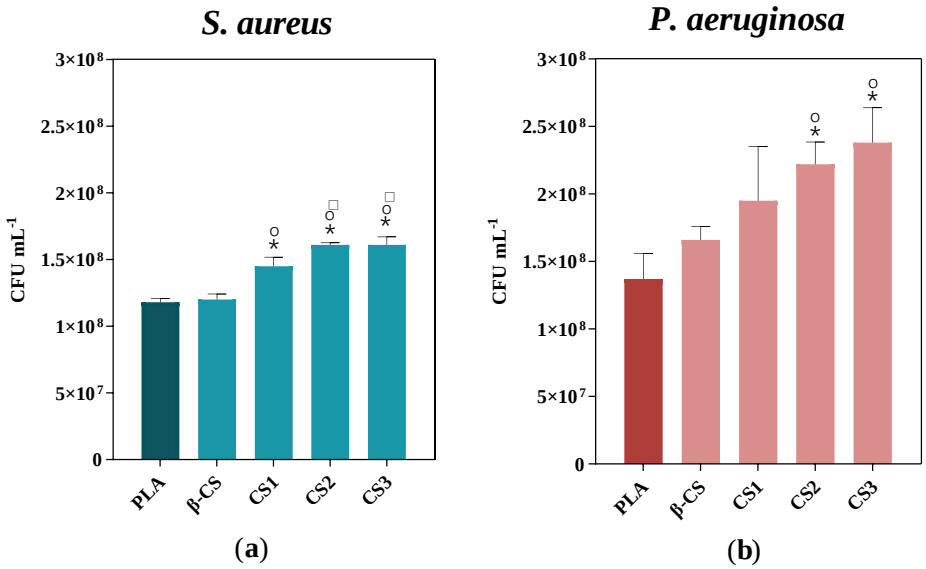


Figure 6. Colony-forming units counting of supernatant of (**a**) *S. aureus* and (**b**) *P. aeruginosa* after 24 h incubation with PLA, PLA-β-CS, PLA-CS1, PLA-CS2 and PLA-CS3 surfaces. Significant differences are considered for *p*-values < 0.05 and represented by *, ○, and □ when compared with PLA, β-CS, and CS1, respectively.

It was also observed that the effect of CS-based surfaces on the composition of the supernatant depended on the MW of immobilized CS. In fact, the concentration of bacteria in the supernatant significantly increased with the decrease of CS MW ($p < 0.05$), which suggests that the MW of the polymer may influence its anti-adhesive activity. In both *S. aureus* and *P. aeruginosa*, the highest bacterial concentrations in the supernatant are associated with the surfaces coated with low MW CS (PLA-CS2 and PLA-CS3 surfaces), which may correspond to the surfaces with the highest antibiofilm activity (as explained above). Additionally, by comparing Figure 6a to Figure 6b, it was observed that CS-based surfaces yielded a different antimicrobial effect against *S. aureus* and *P. aeruginosa* cells. Once again, this result can be explained by the mass balance and the anti-adhesive activity of the CS-based surfaces. Perhaps these surfaces present higher antibiofilm activity against Gram-negative bacteria (such as *P. aeruginosa*) than Gram-positive bacteria, resulting in a lower adhesion of bacteria to the surfaces and, consequently, higher bacterial concentration in the supernatant. Given these results, it became extremely relevant to evaluate the antibiofilm activity of CS-based surfaces.

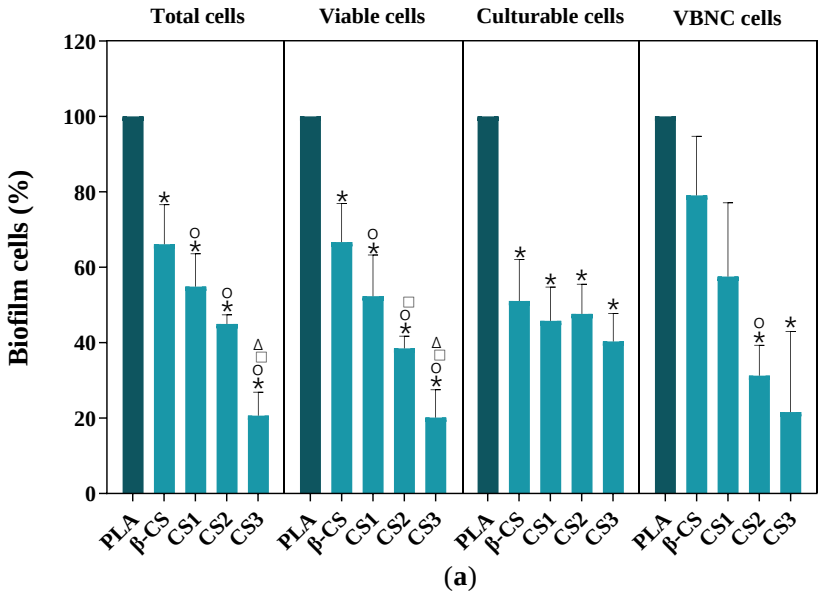
4.2.3. Antibiofilm activity of PLA-CS surfaces

Besides the surface properties, biofilm development may be influenced by the microorganism type [126]. Thus, the efficacy of CS-coated PLA surfaces was assessed against both a Gram-positive (*S. aureus*) and a Gram-negative (*P. aeruginosa*) bacteria, which can easily form biofilm on foreign bodies [36]. To evaluate the antibiofilm activity of the CS-based surfaces against single- and dual-species biofilms of *S. aureus* and *P. aeruginosa*, and the influence of CS MW on this activity, biofilm assays were performed on 12-well microplates by inoculating PLA (control) and CS-based surfaces (PLA-β-CS, PLA-CS1, PLA-CS2 and PLA-CS3) with cell suspensions of *S. aureus*, *P. aeruginosa* and a mixed inoculum (1×10^7 CFU.mL^{-1}). After 24 h of incubation under static conditions, the biofilm composition was analyzed by two methods: CFU counting to determine the number of culturable cells, and epifluorescence microscopy using the Live/Dead kit to determine the number of total and viable cells. The Live/Dead kit consists of a green-fluorescent dye (SYTO®9), which penetrates both intact and damaged membrane cells, and a red-fluorescent dye (PI) that only stains cells with cell membrane damages. Thus, in microscopic images, red-stained cells correspond to the number of non-viable cells, while green-stained cells correspond to the number of viable cells. The number of VBNC cells was determined by the difference between the number of viable and culturable cells. The cellular composition of biofilms is shown in Figure 7, where percentages of total, viable, culturable and VBNC cells of each of CS-based surfaces compared to PLA surfaces are represented.

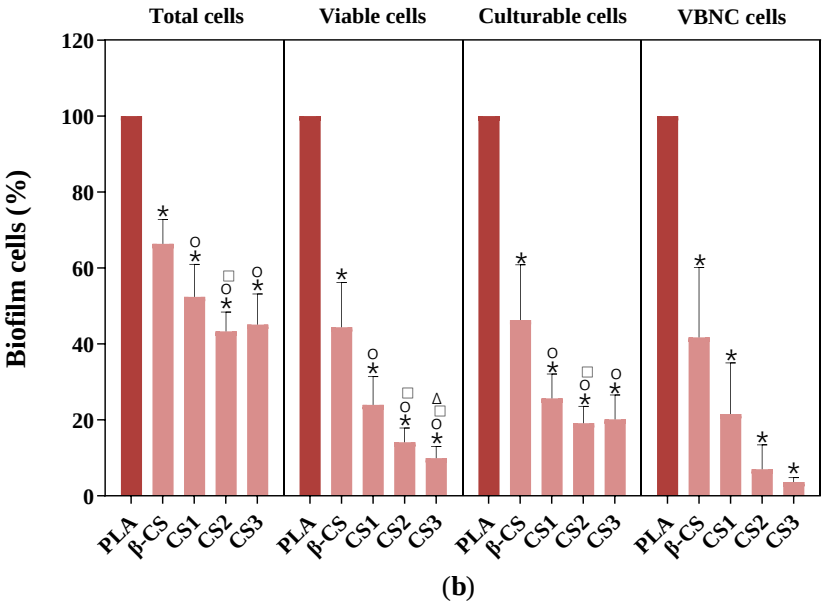
Regarding the composition of 24-h single-species biofilms of *S. aureus* (Figure 7a), the total cell count indicates that CS-based surfaces had about 34-79% fewer cells than PLA surfaces ($p < 0.05$), which reveals the anti-adhesive activity of these surfaces against this Gram-positive bacteria. Moreover, the reduction of the total cell number was significantly higher in PLA-CS surfaces that were coated with the low MW CS, i.e. on PLA-CS2 and PLA-CS3 surfaces ($p < 0.05$), suggesting a weight-dependent effect. The reduction of Gram-positive bacteria adhesion on CS-based surfaces was already reported in a previous study developed by Bulwan et al. [82], in which the anti-adhesive activity of CS against *S. aureus* was demonstrated since CS-coated silicone films suppressed the biofilm formation. Concerning the cellular viability of *S. aureus* biofilms (Figure 7a), a similar tendency was observed since CS-based surfaces allowed reductions between 33-80%, being the most promising ones the PLA-CS2 and PLA-CS3 surfaces ($p < 0.05$). Moreover, the cell culturability of the biofilms developed on CS surfaces was on average 50% lower than on PLA surfaces ($p < 0.05$), revealing the CS antimicrobial properties. The low percentages of viable and culturable cells on PLA-CS surfaces validate what was previously described in the literature regarding the strong antimicrobial activity of CS coatings. According to Kara et al. [69], the surface modification of polyurethane films with 0.5% CS was effective in reducing the viability of *S. aureus* biofilms. Through colony counting assays, authors found that the cellular viability of biofilms developed on CS-surfaces was reduced by 51.7%, compared to the control [69]. VBNC cells are living cells and represent a physiological state adopted by some pathogens when they find adverse external conditions. It is extremely important to consider VBNC cells in clinical

scenarios because these cells are in a dormant state and lose the ability to grow in agar medium, and are not detected by the convention plate count techniques, leading to an incorrect determination of the total number of viable cells [63]. Since they are viable cells, the problem associated with VBNC cells is related to the fact that, under favorable conditions, they can recover their culturability and be responsible for reinfections [132]. The antimicrobial resistance, and the ability of these cells to persist in a given environment and cause reinfections, highlights the need to develop novel strategies/surfaces that decrease the presence of VBNC cells in IMDs. Figure 7a shows that a lower number of VBNC cells was found on CS-based surfaces when compared to the control ($p < 0.05$), and that the PLA surface coated with the lower MW CS (PLA-CS3) allowed a reduction of 78%, being the most promising surface for application in IMDs.

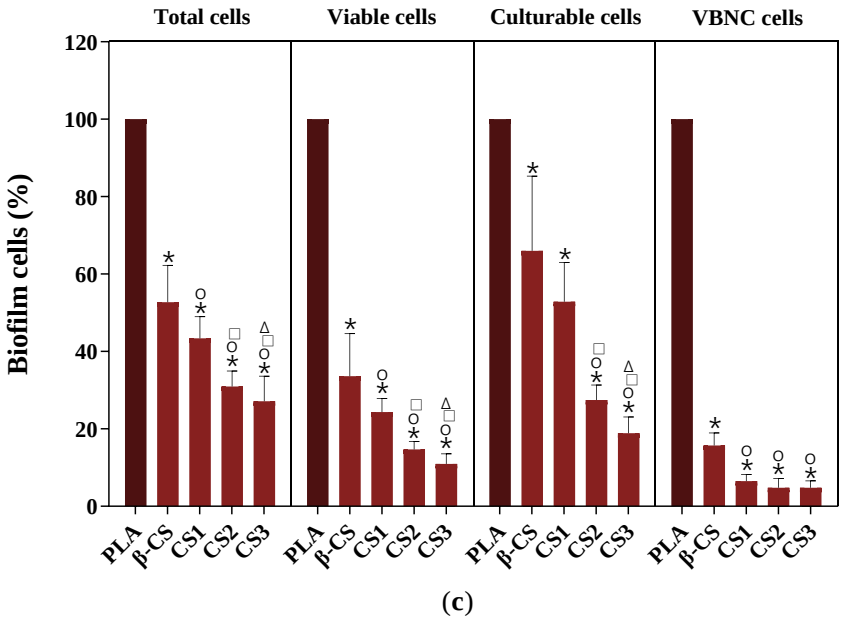
Besides the promising effect against *S. aureus* biofilm formation, the antimicrobial and antibiofilm activities of CS-based surfaces were also evaluated against single-species biofilms of *P. aeruginosa*, which is a Gram-negative bacteria commonly isolated from IAIs [12]. The analysis of biofilm cell composition (Figure 7b) showed that the number of total cells adhered to the CS-coated PLA surfaces was 34-55% lower than observed on uncoated PLA surfaces ($p < 0.05$). Similar to what was observed for *S. aureus* biofilms, with *P. aeruginosa* the anti-adhesive activity of the CS surfaces is also dependent on the MW of CS used in the coating. Results showed that the anti-adhesive effect increases with the decrease of CS MW ($p < 0.05$), being the PLA-CS2 and PLA-CS3 the most promising surfaces. This reduction in the number of bacterial cells adhered to the CS coated surfaces is in agreement with what was observed in a previous study performed by Pandiselvi and Thambidurai [116], in which was revealed that the immobilization of ZnONPs on CS-polyaniline composites effectively inhibited biofilm formation of *P. aeruginosa* by more than 95% [116]. Regarding the viability and culturability of *P. aeruginosa* biofilm cells (Figure 7b), it was observed that, compared to PLA surfaces, only 10-44% of the cells adhered to CS surfaces were viable and that these surfaces reduced the number of culturable cells by 54-80% ($p < 0.05$). Once again, the most promising surfaces were those that were coated with low MW CS (PLA-CS2 and PLA-CS3 surfaces) since they exhibited the lowest percentages of viable and culturable cells ($p < 0.05$). The antimicrobial activity of CS-based surfaces against Gram-negative bacteria was already observed in previous studies. Kara et al. [69] evaluated the antimicrobial activity of CS coatings against *P. aeruginosa* and demonstrated that CS (0.5%)-coated polyurethane films reduced the biofilm viability by 24% compared to the control [69]. Regarding the activity of the tested CS surfaces against VBNC cells (Figure 7b), maximum reductions of 93% and > 96% were verified on PLA-CS2 and PLA-CS3 surfaces, respectively, compared to PLA ($p < 0.05$). As previously explained for *S. aureus* biofilms, such significant reductions in VBNC cell numbers make CS-based surfaces a very promising approach for application in IMDs.


Total cells
Viable cells
Culturable cells
VBNC cells
Biofilm cells (%)
0
20
40
60
80
100
120
PLA
β-CS
CS1
CS2
CS3

(a)


Total cells
Viable cells
Culturable cells
VBNC cells
Biofilm cells (%)
0
20
40
60
80
100
120
PLA
β-CS
CS1
CS2
CS3

(b)


Total cells
Viable cells
Culturable cells
VBNC cells
Biofilm cells (%)
0
20
40
60
80
100
120
PLA
β-CS
CS1
CS2
CS3

(c)

Figure 7. Cellular composition of 24-h single-species biofilms of (**a**) *S. aureus* and (**b**) *P. aeruginosa*, and of (**c**) dual-species biofilms of *S. aureus* and *P. aeruginosa* developed on PLA and CS-based surfaces: percentages of total, viable, culturable and viable but non-culturable (VBNC) cells of biofilms developed on β-CS, CS1, CS2 and CS3 surfaces compared to the control (PLA surfaces). Inferential statistics were performed using the nonparametric Mann-Whitney test and significant differences are represented for *p*-values < 0.05 by *, ○, □, and Δ when compared with PLA, β-CS, CS1, and CS2, respectively.

By comparing the cellular composition of *S. aureus* and *P. aeruginosa* biofilms (Figure 7a,b), namely by the percentages of viable, culturable and VBNC cells, a higher antimicrobial effect of CS surfaces was observed against *P. aeruginosa* biofilms than for *S. aureus* biofilms. The antimicrobial activity of the compounds may depend on the membrane composition of the microorganisms under analysis. As mentioned above, *S. aureus* and *P. aeruginosa* are Gram-positive and Gram-negative bacteria, respectively, and therefore they have a different membrane composition. Gram-positive bacteria only have one cytoplasmic membrane and a very thick wall in which multilayers of peptidoglycan exist. Although the lack of an outer cell membrane may make them more susceptible to antimicrobial compounds, such as CS, the results obtained in this work showed that *S. aureus* biofilms were less susceptible than *P. aeruginosa* biofilms. The higher antimicrobial activity of CS-based surfaces against *P. aeruginosa* can be explained by bacteria surface polarity and the different CS mechanisms of action. One of them states that the inactivation of cells by CS results from the interaction between positively charged CS molecules and negatively charged cell membranes, which can change membrane permeability and lead to cell death [83]. The antimicrobial activity of CS is dependent on the intensity of electrostatic interactions between the polymer and the cell, which depend on the charge density of the surfaces. As the membranes of Gram-negative bacteria are essentially composed of phosphate and pyrophosphate groups, they have a higher negative charge density than Gram-positive bacteria [69]. Thus, the higher number of negative charges on the surface of *P. aeruginosa* cells may justify the stronger electrostatic interactions between these cells and CS and, consequently, the higher antimicrobial activity of CS.

In natural systems, such as the human body, there are no isolated colonies but communities of complex and diverse microorganisms, organized in mixed biofilms. As several studies have reported that these biofilms exhibit higher resistance than single-species biofilms, the antimicrobial and antibiofilm activities of CS-based surfaces were also evaluated against dual-species biofilms of *S. aureus* and *P. aeruginosa*, to mimic conditions found in several clinical scenarios. Figure 7c shows the cellular composition of *S. aureus* and *P. aeruginosa* dual-species biofilms. The analysis of total cells indicates that CS-based surfaces reduced the recoverable adherent bacteria levels by 47-73%, compared to PLA surfaces ($p < 0.05$). Moreover, as verified for single-species biofilms, with the decrease of CS MW, the anti-adhesive activity increased ($p < 0.05$). In fact, PLA-CS2 and PLA-CS3 led to a 69 and 73% reduction of adherent bacteria, being the most promising surfaces. A similar trend was observed for the number of viable and culturable cells, with biofilms formed on CS surfaces presenting less 66-89% and 34-81% of viable and culturable cells compared to the control ($p < 0.05$). Once again, the

antimicrobial activity was significantly higher on the surfaces coated with the lowest MW CS, i.e. on PLA-CS2 and PLA-CS3 surfaces ($p < 0.05$). These two surfaces also exerted the highest reduction in the number of VBNC cells, exhibiting around 95% fewer cells than PLA surfaces ($p < 0.05$). Other authors also demonstrated the efficacy of CS-based surfaces to inhibit dual-species biofilms. Tan et al. [92] demonstrated that CS-coated silicone surfaces inhibited both single- and dual-species biofilms of *S. epidermidis* and *C. albicans*, decreasing dual-species biofilm formation and metabolic activity by 70 and 60%, respectively [92].

By comparing the cellular composition of single-biofilms of *P. aeruginosa* and dual-species biofilms of *S. aureus* and *P. aeruginosa* (Figure 7b,c), namely by the percentages of viable, culturable and VBNC cells, a similarity in the antimicrobial activity of the CS-based surfaces against these two biofilms was detected. This similarity can be explained by the composition of the dual-species biofilms. In fact, by analyzing the proportion of *S. aureus* and *P. aeruginosa* culturable cells in the total number of culturable cells adhered to the surfaces (Figure D-1a-f in Appendix D), it was observed that mixed biofilms were mostly composed of *P. aeruginosa* cells, which represent more than 81% of adhered culturable cells on CS-based surfaces. So, the predominance of *P. aeruginosa* may justify the antimicrobial activity of the CS-based surfaces against mixed cultures.

The antimicrobial and antibiofilm activities of PLA and CS-coated PLA surfaces against single- and dual-species biofilms of *S. aureus* and *P. aeruginosa* were also evaluated by CLSM, which allowed to acquire images of the three-dimensional (3D) structure of the biofilms, as well as quantitative data related to their biovolume and thickness. Figure 8 shows representative images of the biofilm structure of single-species biofilms of *S. aureus* and *P. aeruginosa* formed on PLA and CS-coated PLA surfaces (PLA-β-CS, PLA-CS1, PLA-CS2 and PLA-CS3), while Figure 9 presents the biofilm structure of dual-species biofilms (*S. aureus* + *P. aeruginosa*), elucidating the interactive behavior of the strains when co-cultured for 24 h. Figure 10 illustrates the quantitative data of both single- and dual-species biofilms (biovolume and biofilm thickness).

Regarding the 3D structure of single-species biofilms (Figure 8), both for *S. aureus* (Figure 8a-e) and *P. aeruginosa* (Figure 8f-j), it was possible to visualize that the highest biofilm amount was associated with uncoated PLA surfaces (Figure 8a,f) and that a visible reduction in biofilm density occurred between PLA and PLA surfaces functionalized with CS, revealing the efficacy of CS-coated PLA surfaces to inhibit *S. aureus* and *P. aeruginosa* biofilm formation. Furthermore, similarly to what was observed by the analysis of the biofilm composition, the analysis of the biofilm structure showed that a gradual decrease in biofilm amount and thickness (shadow projection on the right of micrographs represented in Figure 8) was observed as the CS MW decreased, regardless of the bacterial strain tested. In fact, through a visual inspection of microscope images (Figure 8a-e for *S. aureus* and Figure 8f-j for *P. aeruginosa*), less dense and thick biofilms were observed from the surface coated with β-CS (MW of 294 kDa) to the surface with CS3 (MW of 61 kDa). These results were validated by the biovolume and biofilm thickness values obtained for single-species biofilms (Figure 10a-d). *S. aureus* biofilms developed on CS-based surfaces (Figure 10a,b) showed about 37-79% lower amount of biomass than

those developed on PLA surfaces and an average thickness corresponding to 33-63% of the control biofilms ($p < 0.05$). Regarding *P. aeruginosa* biofilms (Figure 10c,d), PLA functionalized surfaces were capable of reducing the biovolume and thickness of biofilms by 39-67% and 31-65%, respectively, when compared to the control surface ($p < 0.05$). Once again, the surfaces coated with the two CS with the lowest MW (PLA-CS2 and PLA-CS3 surfaces) showed the highest percentages of reduction in the amount of biomass and thickness of biofilms formed, being the most promising surfaces for application in medical devices.

Looking at the architectural differences between the 24-h biofilms of *S. aureus* and *P. aeruginosa* (Figure 8), microscopic images revealed that the Gram-negative bacteria strain formed denser and thicker biofilms than the Gram-positive bacteria, regardless of the surface material. By analyzing the qualitative data (Figure 10a-d), it was observed that, on average, compared to PLA surfaces, the most promising CS-based surfaces (PLA-CS2 and PLA-CS3) decreased *P. aeruginosa* biofilm biovolume and thickness by 65 and 57% ($p < 0.05$), respectively, while they showed percentages of *S. aureus* biofilm reduction of 78 and 65%, respectively ($p < 0.05$).

In addition to the analysis of single-species biofilm structure, an analysis of the structure of mixed biofilms was carried out to understand the strains' behavior when co-cultured for 24 h. Concerning the 3D structure, Figure 9 shows representative structures of dual-species biofilms of *S. aureus* and *P. aeruginosa* developed on PLA and CS-coated PLA surfaces. The first line (Figure 9i) shows the dual-species biofilms formed on each surface and the spatial location of each of the studied strains. In fact, the combination of the red and green filters allowed the simultaneous identification of *P. aeruginosa* and *S. aureus* cells, respectively. Regarding the second line (Figure 9ii), it corresponds only to the green filter, allowing the identification of the spatial distribution of *S. aureus* cells within the dual-species biofilms. As observed for the single-species biofilms of *P. aeruginosa*, dual-species biofilms were also dense on all tested surfaces. However, by a visual inspection of the shadow projections on the right of micrographs, it was observed that the mixed biofilms were thicker on the uncoated PLA surfaces than on the PLA surfaces coated with CS. Although the thickness of the biofilms developed on the surfaces coated with the three higher MW CS was practically the same (Figure 9a-d), a slight decrease in thickness was observed on the surface coated with the lowest MW CS, the PLA-CS3 surface (Figure 9e).

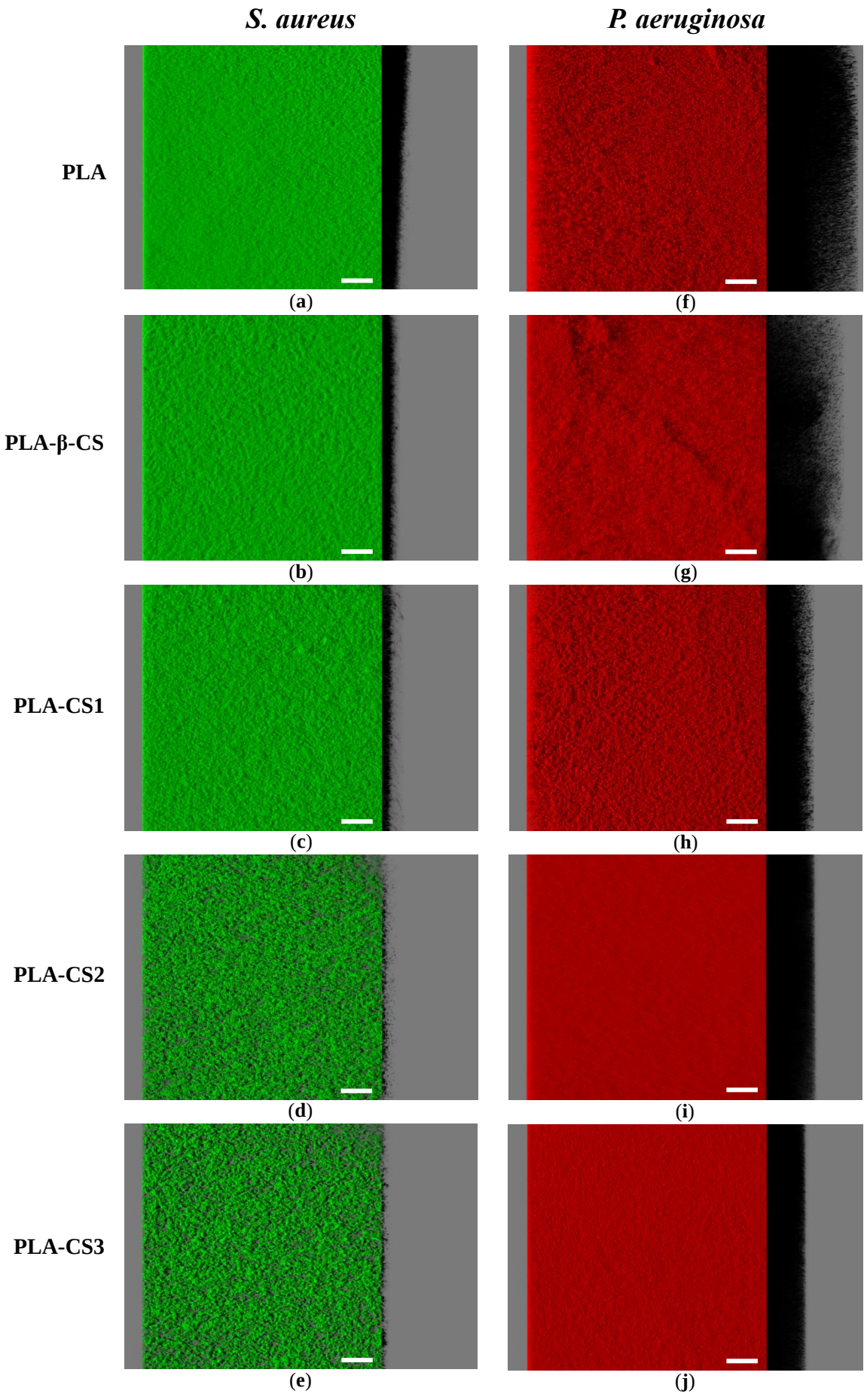

S. aureus
P. aeruginosa
PLA
PLA-β-CS
PLA-CS1
PLA-CS2
PLA-CS3
(a)
(b)
(c)
(d)
(e)
(f)
(g)
(h)
(i)
(j)

Figure 8. Representative biofilm structures of single-species biofilms of (**a-e**) *S. aureus* and (**f-j**) *P. aeruginosa* developed on PLA and synthesized CS surfaces. These images were obtained from CLSM *z*-stacks using IMARIS software and present an aerial, three-dimensional (3D) view of the biofilms (which vertical projections are represented by the shadow on the right). The scale bar is 50 μm.

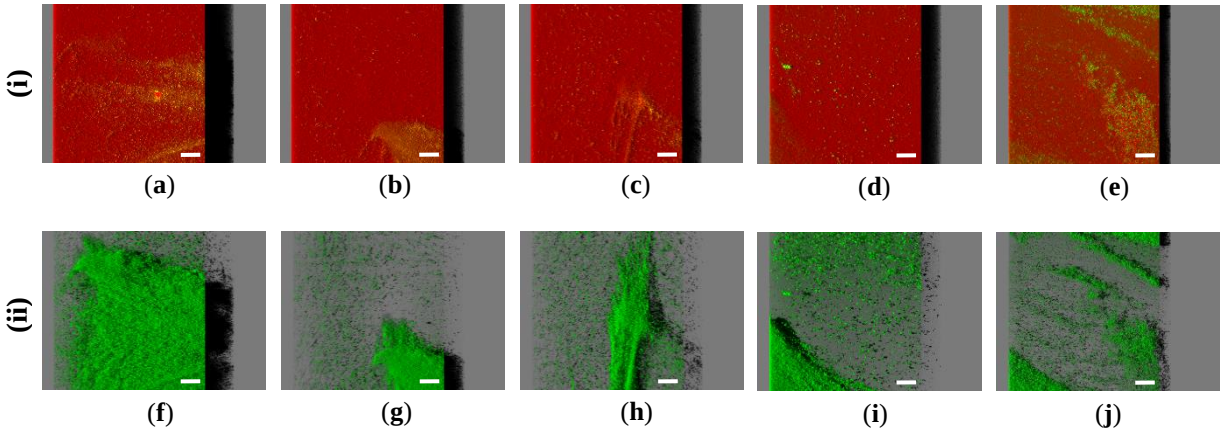


Figure 9. Representative biofilm structures of dual-species biofilms of *S. aureus* and *P. aeruginosa* developed on PLA and synthetized CS surfaces. These images were obtained using IMARIS software and present an aerial view of biofilm structures (which vertical projections are represented by the shadow on the right). The first line (**i**) represents the combination of red and green filters (*S. aureus* + *P. aeruginosa* cells), while the second one (**ii**) corresponds only to the green filter (*S. aureus* cells on dual-species biofilms). The scale bar is 50 μm.

Regarding the composition of the mixed biofilms, by the analysis of Figure 9ii, it was observed that a reduced amount of *S. aureus* cells was heterogeneously distributed over the surfaces, mainly on CS-based surfaces. When comparing the CLSM images of *S. aureus* in single- and dual-species biofilms (Figure 8a-e and Figure 9ii, respectively), it is noticeable that *S. aureus* colonization was reduced in mixed biofilms. In fact, as represented in Figure D-1a-f in Appendix D, *S. aureus* population only represents 14-24% of the total adhered mixed-biofilm cells to CS-based surfaces. Thus, *P. aeruginosa* was the dominant strain, which corroborates what was previously discussed about the similar antimicrobial activity of CS against *P. aeruginosa* and mixed biofilms. Moreover, the CLSM analysis also indicated that, regardless of the tested surface, *S. aureus* and *P. aeruginosa* cells were co-aggregated, which means that they were mixed throughout the biofilm volume (Figure D-2 in Appendix D).

The data of biovolume and biofilm thickness of the dual-species biofilms of *S. aureus* and *P. aeruginosa* (Figure 10e,f) corroborated the previous results of 3D structures. CS-coated surfaces reduced the biovolume and biofilm thickness, on average, to 43 and 52%, respectively, compared to PLA film ($p < 0.05$). Once again, the most promising surface was the one that was coated with the lowest MW CS, i.e. the PLA-CS3 surface ($p < 0.05$). Considering that biofilms developed on implant surfaces are usually composed of more than one strain of pathogenic bacteria, the high antimicrobial and antibiofilm activities of CS-based surfaces against dual-species biofilms make these surfaces, particularly the PLA-CS3 surface, very promising for clinical applications.

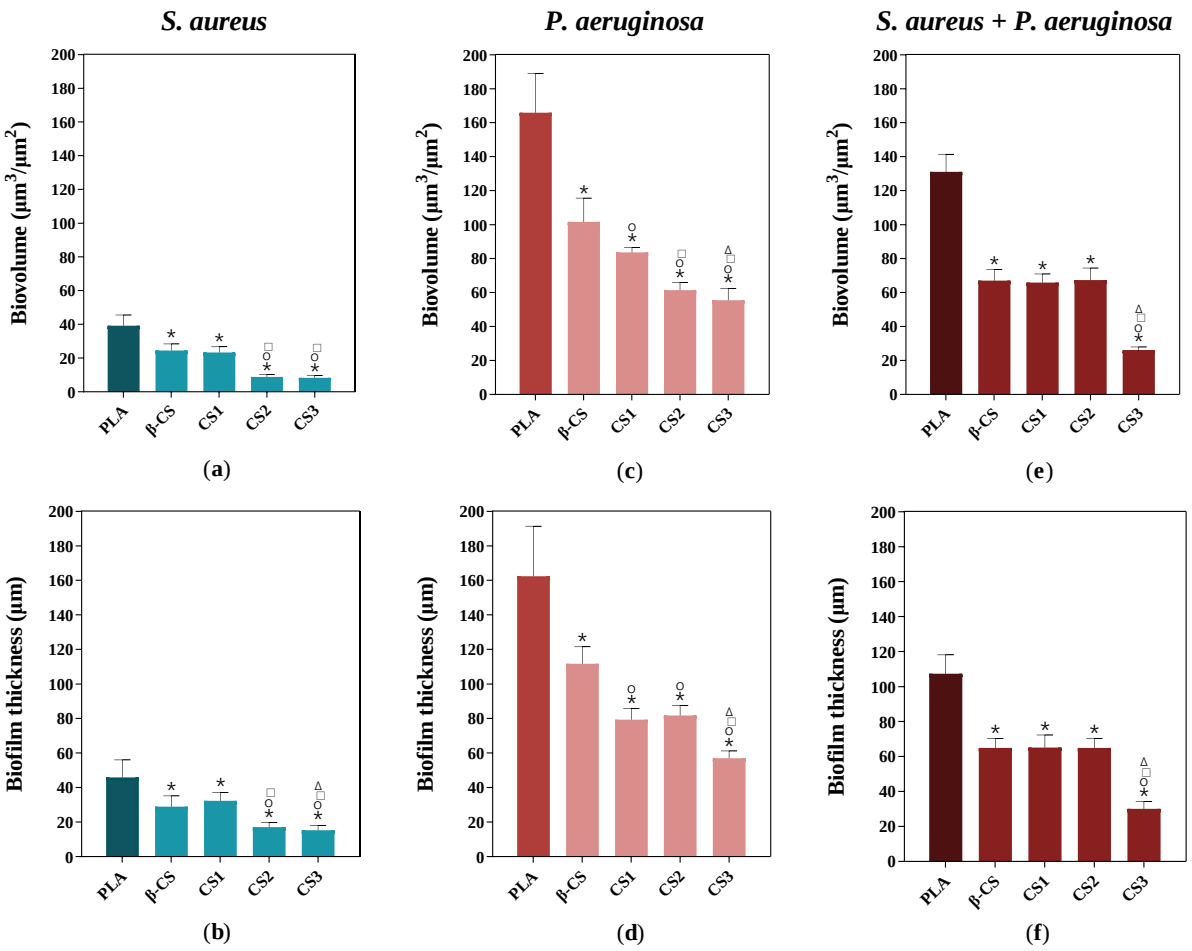


Figure 10. Biovolumes and thickness of (**a-b**) *S. aureus* and (**c-d**) *P. aeruginosa* single-species biofilms, and of (**e-f**) dual-species biofilms (*S. aureus* + *P. aeruginosa*) developed on PLA and synthesized CS surfaces. The values of these parameters were estimated from CLSM *z*-stacks using the COMSTAT2 tool associated with the ImageJ software, and the means ± standard deviations result from three independent assays. A one-way analysis of variance (ANOVA) was used to perform a statistical analysis and significant differences were represented for *p*-values < 0.05 by *, ○, □, and Δ when compared with PLA, β-CS, CS1, and CS2, respectively.

Overall, by analyzing the biofilm cell composition and biofilm structure, it was observed that the CS-based surfaces showed a high anti-adhesive and antibiofilm activity against single- and dual-species biofilms of *S. aureus* and *P. aeruginosa*, allowing significant reductions in the number of total, viable, culturable and VBNC cells. A possible explanation for the anti-adhesive activity of CS-based surfaces can be related to the increased hydrophilicity of PLA surfaces when they are coated with CS (as demonstrated previously in Section 4.2.1.). Indeed, CS molecules increase the number of polar groups, reducing microbial adhesion of both Gram-positive and Gram-negative bacteria. Regarding the antimicrobial activity, CS-coated PLA surfaces significantly reduced viable and culturable cells, being this effect more pronounced in *P. aeruginosa* biofilms than in *S. aureus* biofilms, which can be explained by the CS' mechanism of action and the different charge densities of bacteria surfaces.

Furthermore, as demonstrated by the biofilm cell composition and structure, the antimicrobial activity of functionalized PLA surfaces depends on the CS MW used in the coating, regardless of the

strain tested. PLA-CS2 and PLA-CS3 surfaces (coated with the lower MW CS, 129 and 61 kDa, respectively) were the most promising surfaces for reducing the number of biofilm cells. One of the proposed mechanisms of action for this natural polymer is based on the ability of CS molecules to cross the membrane and bind to DNA, inhibiting RNA synthesis and consequent protein synthesis [79]. Thus, the enhanced antimicrobial activity of PLA-CS2 and PLA-CS3 surfaces can be justified by the higher and easier penetration of low MW CS molecules into the bacterial membranes due to their reduced size [133]. In addition, the highest surface homogeneity of PLA surfaces coated with low MW CS may have contributed to the higher anti-adhesive and antibiofilm effect on these surfaces. The decreased number of small aggregates of CS in PLA-CS3 surfaces may have increased the contact area between the bacteria and the CS molecules, increasing the effectiveness of CS-based surfaces.

Regarding VBNC cells, it was observed that PLA surfaces coated with CS were highly effective in reducing this type of biofilm cells, since they allowed reduction percentages higher than 96% compared to uncoated PLA films. VBNC cells are a concern for the clinical area. Besides offering higher resistance to antibiotic treatments and human defenses, these cells can regain culturability and cause reinfections, reason why it is crucial to find effective strategies against VBNCs. To the best of our knowledge, the present work is the first to study the effect of CS-coated surfaces on the reduction of the number of VNBCs and whose results suggest that coating implants with CS may be a very promising strategy.

The clear antimicrobial and antibiofilm activity of CS-based surfaces against both single- and dual-species biofilms of *S. aureus* and *P. aeruginosa* demonstrates the potential of CS use for medical applications, namely for the coating of IMDs to reduce IAIs.

5. Conclusion

Concurrently with the increase in the number of implanted devices, the medical field has been faced with an increase in the number of IAIs. Microbial colonization and biofilm formation on implant surfaces has limited the strategies used to treat these infections, encouraging the development of innovative antimicrobial biomaterials.

The systematic review of the literature developed in this work showed that, in the last years, there has been a growing interest in the use of CS for surface engineering due to its biological properties. The review investigated the potential of CS (functionalized and non-functionalized) and CS in association with other compounds (antimicrobial agents, metals and polymers) to effectively reduce bacterial and fungal adhesion and, consequently, biofilm formation. Data demonstrated that surfaces modified with CS composites exhibited a strong anti-adhesive and antibiofilm activity against a broad spectrum of pathogenic microorganisms, encouraging the use of CS for the coating of IMDs.

The results of the experimental component of this work demonstrated the high antimicrobial and antibiofilm activity of CS-based surfaces against single- and dual-species biofilms of *S. aureus* and *P. aeruginosa*, being these activities dependent on the CS MW. In fact, the most promising surface was that contained the CS with lower MW since it exhibited the highest antibiofilm activity, as verified by the analysis of the biofilm composition and structure. Therefore, bioengineering of CS-based surfaces may be a promising approach for the coating of IMDs since these surfaces present the required antimicrobial and antibiofilm activities for the prevention of IAIs. Furthermore, the use of CS enables the valorization of fish processing industry waste, being an economically and environmentally sustainable strategy.

6. Outputs

The current project was developed in the last three months in collaboration with International Iberian Nanotechnology Laboratory (INL, Braga) and Grupo de Reciclado y Valorización de Materiales Residuales (REVAL) - Instituto de Investigaciones Marinas (IIM-CSIC, Spain).

In March 2021, this project entitled "Chitosan-based surfaces to prevent implant-associated infections" was accepted for oral presentation in Science Under 5', at the 12th Symposium of Bioengineering at the Faculty of Engineering of the University of Porto.

Later, in May 2021, an abstract entitled "Antimicrobial surfaces based on chitosan to prevent implant-associated infections" was accepted for oral presentation at the 14th Young Researchers Meeting of the University of Porto (IJUP), whose book of abstracts was published (ISBN: 978-989-746-295-5).

Furthermore, in May 2021, a review article entitled "Antimicrobial coatings based on chitosan to prevent implant-associated infections: a systematic review" was submitted in *iScience* journal based on the topics analyzed in the present systematic review of the literature, and is currently under review. Moreover, in the same month, an article manuscript entitled "Development of Chitosan-Based Surfaces to Prevent Single- and Dual-Species Biofilms of *Staphylococcus aureus* and *Pseudomonas aeruginosa*" was prepared from the experimental results obtained in this dissertation project and is already published in *Molecules* journal (doi: 10.3390/molecules26144378).

7. Future perspectives

As future work concerning the systematic review of the literature, it would be interesting to assess the methodological quality and potential bias of the selected studies, which can be done through a Methodological Index for Non-Randomized Studies (MINORS) scale. Although this scale is not suitable for the analysis of laboratory studies, an adaptation to the specific context could be made (MINORS scale for *in vitro* studies) in order to assess the predictive value of the studies and identify promising clinical applications. Moreover, a meta-analysis of the data obtained could be carried out.

Regarding the CS-based surfaces, this study demonstrated their efficacy in reducing bacterial adhesion and single- and dual-species biofilm formation of *S. aureus* and *P. aeruginosa*. However, in natural systems such as the human body, microorganisms are organized in complex and diverse communities, which are not only composed of bacteria. Furthermore, in future work, the antimicrobial and antibiofilm activity of the tested CS-surfaces will also be assessed against *C. albicans*, which can be considered as a representative model yeast since it is typically isolated from IAIs [12]. Additionally, it should be noticed that all the strains selected and evaluated are reference collection strains, so they may not reflect the physiology and biofilm formation of the pathogenic strains commonly found in humans. Hence, additional assays could be performed using clinical isolates of an implanted device to mimic more closely the conditions to which IMDs are subjected in the human body.

Whereas the antimicrobial activity of CS is dependent on many factors of which only the CS MW was assessed, in future work, the effect of CS concentration will also be evaluated. For that, surfaces with 1% (w/v) CS will be produced and their performance to reduce bacterial adhesion and biofilm formation evaluated under the same conditions used for 0.5% (w/v) CS-surfaces.

Given the results obtained by the systematic literature review, in the last years, the association of CS with other compounds has been widely studied to prevent bacterial adhesion and biofilm formation in IMDs. Thus, as future work, it would be interesting to associate the lowest MW CS (CS3) with other antimicrobial compounds and evaluate the anti-adhesive and antibiofilm activities of this combination. Functionalization of low MW chitosans will also be pursued.

Additionally, *in vitro* studies using cell lines (cytotoxicity assays) and *in vivo* assays with animal models are needed to understand the clinical performance of CS and its derivatives so that they can be effectively and safely used in medical applications.

References

1. Vinh, D.C. and J.M. Embil, *Device-related infections: a review.* J. Long Term Eff. Med. Implants, 2005. **15**(5): p. 467-88.
2. Kuehl, R., et al., *Preventing Implant-Associated Infections by Silver Coating.* Antimicrob. Agents Chemother., 2016. **60**(4): p. 2467-2475.
3. D'Almeida, M., et al., *Chitosan coating as an antibacterial surface for biomedical applications.* PLoS One, 2017. **12**(12): p. e0189537.
4. Tande, A.J. and R. Patel, *Prosthetic joint infection.* Clin. Microbiol. Rev., 2014. **27**(2): p. 302-345.
5. Darouiche, R.O., *Device-associated infections: a macroproblem that starts with microadherence.* Clin. Infect. Dis., 2001. **33**(9): p. 1567-72.
6. Orapiriyakul, W., et al., *Antibacterial surface modification of titanium implants in orthopaedics.* J. Tissue Eng., 2018. **9**: p. 2041731418789838.
7. Khatoon, Z., et al., *Bacterial biofilm formation on implantable devices and approaches to its treatment and prevention.* Heliyon, 2018. **4**(12): p. e01067.
8. Adlhart, C., et al., *Surface modifications for antimicrobial effects in the healthcare setting: a critical overview.* J. Hosp. Infect., 2018. **99**(3): p. 239-249.
9. Zhu, Z., et al., *Antimicrobial strategies for urinary catheters.* J. Biomed. Mater. Res. A, 2019. **107**(2): p. 445-467.
10. Oyatogun, G.M., et al., *Chapter 11 - Chitin, chitosan, marine to market*, in *Handbook of Chitin and Chitosan*, S. Gopi, S. Thomas, and A. Pius, Editors. 2020, Elsevier. p. 341-381.
11. Tipnis, N.P. and D.J. Burgess, *Sterilization of implantable polymer-based medical devices: A review.* Int. J. Pharm., 2018. **544**(2): p. 455-460.
12. Kandi, V. and S. Vadakedath, *Implant-Associated Infections: A Review of the Safety of Cardiac Implants.* Cureus, 2020. **12**(12): p. e12267-e12267.
13. Domb, A. and W. Khan, *Focal Controlled Drug Delivery*. 2014.
14. Darouiche, R.O., *Treatment of infections associated with surgical implants.* N. Engl. J. Med., 2004. **350**(14): p. 1422-9.
15. Market Data Forecast. *Active Implantable Medical Devices Market*. 2020. [Online]; Available from: https://www.marketdataforecast.com/market-reports/active-implantable-medical-devices-market.
16. Bryers, J.D., *Medical biofilms.* Biotechnol. Bioeng., 2008. **100**(1): p. 1-18.
17. Trampuz, A. and A.F. Widmer, *Infections associated with orthopedic implants.* Curr. Opin. Infect. Dis., 2006. **19**(4): p. 349-56.
18. VanEpps, J.S. and J.G. Younger, *Implantable Device-Related Infection.* Shock, 2016. **46**(6): p. 597-608.

19. Hetrick, E.M. and M.H. Schoenfisch, *Reducing implant-related infections: active release strategies.* Chem. Soc. Rev., 2006. **35**(9): p. 780-9.

20. Costerton, J.W., et al., *Bacterial biofilms in nature and disease.* Annu. Rev. Microbiol., 1987. **41**: p. 435-64.

21. Campana, R., et al., *Chitosans as new tools against biofilms formation on the surface of silicone urinary catheters.* Int. J. Biol. Macromol., 2018. **118**(Pt B): p. 2193-2200.

22. Costerton, J.W., P.S. Stewart, and E.P. Greenberg, *Bacterial biofilms: a common cause of persistent infections.* Science, 1999. **284**(5418): p. 1318-22.

23. Donlan, R.M., *Biofilms: microbial life on surfaces.* Emerg. Infect. Dis., 2002. **8**(9): p. 881-90.

24. Floyd, K.A., A.R. Eberly, and M. Hadjifrangiskou, *3 - Adhesion of bacteria to surfaces and biofilm formation on medical devices*, in *Biofilms and Implantable Medical Devices*, Y. Deng and W. Lv, Editors. 2017, Woodhead Publishing. p. 47-95.

25. Singha, P., J. Locklin, and H. Handa, *A review of the recent advances in antimicrobial coatings for urinary catheters.* Acta Biomater., 2017. **50**: p. 20-40.

26. Deva, A.K., W.P. Adams, Jr., and K. Vickery, *The role of bacterial biofilms in device-associated infection.* Plast. Reconstr. Surg., 2013. **132**(5): p. 1319-1328.

27. Azevedo, A.S., et al., *Impact of polymicrobial biofilms in catheter-associated urinary tract infections.* Crit. Rev. Microbiol., 2017. **43**(4): p. 423-439.

28. Arciola, C.R., D. Campoccia, and L. Montanaro, *Implant infections: adhesion, biofilm formation and immune evasion.* Nat. Rev. Microbiol., 2018. **16**(7): p. 397-409.

29. Harris, L.G. and R.G. Richards, *Staphylococci and implant surfaces: a review.* Injury, 2006. **37 Suppl 2**: p. S3-14.

30. Anju, V.T., et al., *Malachite green-conjugated multi-walled carbon nanotubes potentiate antimicrobial photodynamic inactivation of planktonic cells and biofilms of Pseudomonas aeruginosa and Staphylococcus aureus.* Int. J. Nanomed., 2019. **14**: p. 3861-3874.

31. Donlan, R.M. and J.W. Costerton, *Biofilms: survival mechanisms of clinically relevant microorganisms.* Clin. Microbiol. Rev., 2002. **15**(2): p. 167-93.

32. Penesyan, A., M. Gillings, and I.T. Paulsen, *Antibiotic discovery: combatting bacterial resistance in cells and in biofilm communities.* Molecules, 2015. **20**(4): p. 5286-98.

33. Mulcahy, L.R., et al., *Emergence of Pseudomonas aeruginosa strains producing high levels of persister cells in patients with cystic fibrosis.* J. Bacteriol., 2010. **192**(23): p. 6191-9.

34. Sun, F., et al., *Biofilm-associated infections: antibiotic resistance and novel therapeutic strategies.* Future Microbiol., 2013. **8**(7): p. 877-86.

35. Schierholz, J.M. and J. Beuth, *Implant infections: a haven for opportunistic bacteria.* J. Hosp. Infect., 2001. **49**(2): p. 87-93.

36. Veerachamy, S., et al., *Bacterial adherence and biofilm formation on medical implants: a review.* Proc. Inst. Mech. Eng. H, 2014. **228**(10): p. 1083-99.

37. Younes, I. and M. Rinaudo, *Chitin and chitosan preparation from marine sources. Structure, properties and applications.* Mar. Drugs, 2015. **13**(3): p. 1133-74.

38. Yi, H., et al., *Biofabrication with chitosan.* Biomacromolecules, 2005. **6**(6): p. 2881-94.

39. Tolaimate, A., et al., *On the influence of deacetylation process on the physicochemical characteristics of chitosan from squid chitin.* Polymer, 2000. **41**(7): p. 2463-2469.

40. Gomes, L.C., et al., *The Effect of Molecular Weight on the Antimicrobial Activity of Chitosan from Loligo opalescens for Food Packaging Applications.* Mar. Drugs, 2021. **19**(7).

41. Zeidberg, L., *Doryteuthis opalescens, opalescent inshore squid.* Advances in Squid Biology, Ecology and Fisheries. Part I - Myopsid squids, 2013: p. 159-204.

42. Yan, N. and X. Chen, *Sustainability: Don't waste seafood waste.* Nature, 2015. **524**(7564): p. 155-157.

43. Hülsey, M., *Shell biorefinery: A comprehensive introduction.* Green Energy & Environment, 2018. **3**.

44. Tikhonov, V., et al., *Bactericidal and antifungal activities of a low molecular weight chitosan and its N-/2(3)-(dodec-2-enyl)succinoyl/-derivatives.* Carbohydr. Polym., 2006. **64**: p. 66-72.

45. Patrulea, V., et al., *Chitosan as a starting material for wound healing applications.* Eur. J. Pharm. Biopharm., 2015. **97**(Pt B): p. 417-26.

46. Tan, H., et al., *Gelatin/chitosan/hyaluronan scaffold integrated with PLGA microspheres for cartilage tissue engineering.* Acta Biomater., 2009. **5**(1): p. 328-37.

47. Feng, P., et al., *Chitosan-Based Functional Materials for Skin Wound Repair: Mechanisms and Applications.* Front. Bioeng. Biotechnol., 2021. **9**: p. 650598.

48. Li, J., et al., *Chitosan-Based Nanomaterials for Drug Delivery.* Molecules, 2018. **23**(10).

49. Chandrasekaran, M., K.D. Kim, and S.C. Chun, *Antibacterial Activity of Chitosan Nanoparticles: A Review.* Processes, 2020. **8**(9).

50. Li, Z., F. Yang, and R. Yang, *Synthesis and characterization of chitosan derivatives with dual-antibacterial functional groups.* Int. J. Biol. Macromol., 2015. **75**: p. 378-87.

51. Hosseinnejad, M. and S.M. Jafari, *Evaluation of different factors affecting antimicrobial properties of chitosan.* Int. J. Biol. Macromol., 2016. **85**: p. 467-75.

52. Chung, Y.C. and C.Y. Chen, *Antibacterial characteristics and activity of acid-soluble chitosan.* Bioresour. Technol., 2008. **99**(8): p. 2806-14.

53. Kong, M., et al., *Antimicrobial properties of chitosan and mode of action: a state of the art review.* Int. J. Food Microbiol., 2010. **144**(1): p. 51-63.

54. Moher, D., et al., *Preferred reporting items for systematic reviews and meta-analyses: the PRISMA statement.* Ann. Intern. Med., 2009. **151**(4): p. 264-9, w64.

55. Vázquez, J.A., et al., *An integral and sustainable valorisation strategy of squid pen by-products.* J. Clean. Prod., 2018. **201**: p. 207-218.

56. Allan, G.G. and M. Peyron, *Molecular weight manipulation of chitosan. I: Kinetics of depolymerization by nitrous acid.* Carbohydr. Res., 1995. **277**(2): p. 257-72.

57. Pinheiro, A., et al., *K-carrageenan/chitosan nanolayered coating for controlled release of a model bioactive compound.* Innov. Food Sci. Emerg. Technol., 2012. **16**: p. 227-232.

58. da Silva, D., et al., *Biocompatibility, biodegradation and excretion of polylactic acid (PLA) in medical implants and theranostic systems.* Chem. Eng. J., 2018. **340**: p. 9-14.

59. Rajendra, P.P., et al., *Biomedical Applications of Poly(Lactic Acid).* Regen. Med., 2014. **4**(1): p. 40-51.

60. Sezonov, G., D. Joseleau-Petit, and R. D'Ari, *Escherichia coli physiology in Luria-Bertani broth.* J. Bacteriol., 2007. **189**(23): p. 8746-9.

61. Ramstedt, M., et al., *Evaluating Efficacy of Antimicrobial and Antifouling Materials for Urinary Tract Medical Devices: Challenges and Recommendations.* Macromol. Biosci., 2019. **19**(5): p. e1800384.

62. Gomes, M., et al., *Optimizing CNT Loading in Antimicrobial Composites for Urinary Tract Application.* Appl. Sci., 2021. **11**(9).

63. Li, L., et al., *The importance of the viable but non-culturable state in human bacterial pathogens.* Front. Microbiol., 2014. **5**: p. 258.

64. Rosenberg, M., N.F. Azevedo, and A. Ivask, *Propidium iodide staining underestimates viability of adherent bacterial cells.* Sci. Rep., 2019. **9**(1): p. 6483.

65. Gomes, L.C., et al., *Escherichia coli adhesion, biofilm development and antibiotic susceptibility on biomedical materials.* J. Biomed. Mater. Res. A, 2015. **103**(4): p. 1414-23.

66. Alves, P., et al., *The potential advantages of using a poly(HPMA) brush in urinary catheters: effects on biofilm cells and architecture.* Colloids Surf. B, 2020. **191**: p. 110976.

67. Heydorn, A., et al., *Quantification of biofilm structures by the novel computer program COMSTAT.* Microbiology, 2000. **146 (Pt 10)**: p. 2395-2407.

68. Gupta, P., et al., *Biofilm, pathogenesis and prevention--a journey to break the wall: a review.* Arch. Microbiol., 2016. **198**(1): p. 1-15.

69. Kara, F., et al., *Synthesis and surface modification of polyurethanes with chitosan for antibacterial properties.* Carbohydr. Polym., 2014. **112**: p. 39-47.

70. Teixeira-Santos, R., et al., *Antimicrobial and anti-adhesive properties of carbon nanotube-based surfaces for medical applications: a systematic review.* iScience, 2021. **24**(1): p. 102001.

71. Carvalho, F.M., et al., *The Use of Probiotics to Fight Biofilms in Medical Devices: A Systematic Review and Meta-Analysis.* Microorganisms, 2020. **9**(1).

72. M. Gomes, L.C.G., R. Teixeira-Santos and F. J. Mergulhão, *Chapter 3. PDMS in Urinary Tract Devices: Applications, Problems and Potential Solutions*, in *Polydimethylsiloxane: Structure and Applications*, P.N. Carlsen, Editor. 2020, Nova Science Publishers.

73. Ramstedt, M., et al., *Evaluating Efficacy of Antimicrobial and Antifouling Materials for Urinary Tract Medical Devices: Challenges and Recommendations.* Macromol. Biosci., 2019. **19**(5): p. e1800384.

74. Francolini, I., et al., *Antifouling and antimicrobial biomaterials: an overview.* Apmis, 2017. **125**(4): p. 392-417.

75. Martinez, L.R., et al., *Demonstration of antibiofilm and antifungal efficacy of chitosan against candidal biofilms, using an in vivo central venous catheter model.* J. Infect. Dis., 2010. **201**(9): p. 1436-40.

76. Martinez, L.R., et al., *The use of chitosan to damage Cryptococcus neoformans biofilms.* Biomaterials, 2010. **31**(4): p. 669-79.

77. Rabea, E.I., et al., *Chitosan as antimicrobial agent: applications and mode of action.* Biomacromolecules, 2003. **4**(6): p. 1457-65.

78. Pu, Y., et al., *In vitro damage of Candida albicans biofilms by chitosan.* Exp. Ther. Med., 2014. **8**(3): p. 929-934.

79. Sudarshan, N.R., D.G. Hoover, and D. Knorr, *Antibacterial action of chitosan.* Food Biotechnol., 1992. **6**(3): p. 257-272.

80. Jung, B.-O., et al., *Preparation of amphiphilic chitosan and their antimicrobial activities.* J. Appl. Polym. Sci., 1999. **72**(13): p. 1713-1719.

81. Savard, T., et al., *Antimicrobial action of hydrolyzed chitosan against spoilage yeasts and lactic acid bacteria of fermented vegetables.* J. Food Prot., 2002. **65**(5): p. 828-33.

82. Bulwan, M., et al., *Chitosan-based ultrathin films as antifouling, anticoagulant and antibacterial protective coatings.* J. Biomater. Sci. Polym. Ed., 2012. **23**(15): p. 1963-80.

83. Kong, M., et al., *Antibacterial mechanism of chitosan microspheres in a solid dispersing system against E. coli.* Colloids Surf. B, 2008. **65**(2): p. 197-202.

84. Costa, E.M., et al., *Chitosan as an effective inhibitor of multidrug resistant Acinetobacter baumannii.* Carbohydr. Polym., 2017. **178**: p. 347-351.

85. Campana, R., et al., *Chitosans inhibit the growth and the adhesion of Klebsiella pneumoniae and Escherichia coli clinical isolates on urinary catheters.* Int. J. Antimicrob. Agents, 2017. **50**(2): p. 135-141.

86. Magesh, H., et al., *Identification of natural compounds which inhibit biofilm formation in clinical isolates of Klebsiella pneumoniae.* Indian J. Exp. Biol., 2013. **51**(9): p. 764-72.

87. Rubini, D., B.N. Vedha Hari, and P. Nithyanand, *Chitosan coated catheters alleviates mixed species biofilms of Staphylococcus epidermidis and Candida albicans.* Carbohydr. Polym., 2021. **252**: p. 117192.

88. Cobrado, L., et al., *Cerium, chitosan and hamamelitannin as novel biofilm inhibitors?* J. Antimicrob. Chemother., 2012. **67**(5): p. 1159-62.

89. Cobrado, L., et al., *In vivo antibiofilm effect of cerium, chitosan and hamamelitannin against usual agents of catheter-related bloodstream infections.* J. Antimicrob. Chemother., 2013. **68**(1): p. 126-130.

90. Wang, R., et al., *Inhibition of Escherichia coli and Proteus mirabilis adhesion and biofilm formation on medical grade silicone surface.* Biotechnol. Bioeng., 2012. **109**(2): p. 336-45.

91. Tan, Y., et al., *Antibiofilm activity of carboxymethyl chitosan on the biofilms of non-Candida albicans Candida species.* Carbohydr. Polym., 2016. **149**: p. 77-82.

92. Tan, Y., et al., *Inhibition of mixed fungal and bacterial biofilms on silicone by carboxymethyl chitosan.* Colloids Surf. B, 2016. **148**: p. 193-199.

93. Tan, Y., et al., *Efficacy of carboxymethyl chitosan against Candida tropicalis and Staphylococcus epidermidis monomicrobial and polymicrobial biofilms.* Int. J. Biol. Macromol., 2018. **110**: p. 150-156.

94. Fei Liu, X., et al., *Antibacterial action of chitosan and carboxymethylated chitosan.* J. Appl. Polym. Sci., 2001. **79**(7): p. 1324-1335.

95. Peng, Z.-X., et al., *Adjustment of the antibacterial activity and biocompatibility of hydroxypropyltrimethyl ammonium chloride chitosan by varying the degree of substitution of quaternary ammonium.* Carbohydr. Polym., 2010. **81**(2): p. 275-283.

96. Tan, H., et al., *The use of quaternised chitosan-loaded PMMA to inhibit biofilm formation and downregulate the virulence-associated gene expression of antibiotic-resistant staphylococcus.* Biomaterials, 2012. **33**(2): p. 365-77.

97. Niemczyk, A., et al., *Biofunctional catheter coatings based on chitosan-fatty acids derivatives.* Carbohydr. Polym., 2019. **225**: p. 115263.

98. Tan, Y., et al., *Long-term antibiofilm activity of carboxymethyl chitosan on mixed biofilm on silicone.* Laryngoscope, 2016. **126**(12): p. E404-E408.

99. Yuan, S., et al., *Enhancing antibacterial activity of surface-grafted chitosan with immobilized lysozyme on bioinspired stainless steel substrates.* Colloids Surf. B, 2013. **106**: p. 11-21.

100. Ajdnik, U., et al., *Functionalisation of Silicone by Drug-Embedded Chitosan Nanoparticles for Potential Applications in Otorhinolaryngology.* Materials, 2019. **12**(6): p. 847.

101. Cao, Z. and Y. Sun, *Chitosan-based rechargeable long-term antimicrobial and biofilm-controlling systems.* J. Biomed. Mater. Res. A, 2009. **89**(4): p. 960-7.

102. Zhou, W., et al., *Novel pH-responsive tobramycin-embedded micelles in nanostructured multilayer-coatings of chitosan/heparin with efficient and sustained antibacterial properties.* Mater. Sci. Eng. C, 2018. **90**: p. 693-705.

103. Valverde, A., et al., *Antibacterial hyaluronic acid/chitosan multilayers onto smooth and micropatterned titanium surfaces.* Carbohydr. Polym., 2019. **207**: p. 824-833.

104. Tan, Y., et al., *Co-immobilization of cellobiose dehydrogenase and deoxyribonuclease I on chitosan nanoparticles against fungal/bacterial polymicrobial biofilms targeting both biofilm matrix and microorganisms.* Mater. Sci. Eng. C, 2020. **108**: p. 110499.

105. Elchinger, P.-H., et al., *Immobilization of proteases on chitosan for the development of films with anti-biofilm properties.* Int. J. Biol. Macromol., 2015. **72**: p. 1063-1068.

106. Raman, N., et al., *Intraluminal Release of an Antifungal β-Peptide Enhances the Antifungal and Anti-Biofilm Activities of Multilayer-Coated Catheters in a Rat Model of Venous Catheter Infection.* ACS Biomater. Sci. Eng., 2016. **2**(1): p. 112-121.

107. Rodríguez López, A.L., et al., *Preventing S. aureus biofilm formation on titanium surfaces by the release of antimicrobial β-peptides from polyelectrolyte multilayers.* Acta Biomater., 2019. **93**: p. 50-62.

108. Monteiro, C., et al., *AMP–Chitosan Coating with Bactericidal Activity in the Presence of Human Plasma Proteins.* Molecules, 2020. **25**(13).

109. Vilcacundo, R., et al., *Antibacterial Activity of Hen Egg White Lysozyme Denatured by Thermal and Chemical Treatments.* Sci. Pharm., 2018. **86**(4).

110. Elchinger, P.H., et al., *Effect of proteases against biofilms of Staphylococcus aureus and Staphylococcus epidermidis.* Lett. Appl. Microbiol., 2014. **59**(5): p. 507-13.

111. Shenkman, B., et al., *Role of agr (RNAIII) in Staphylococcus aureus adherence to fibrinogen, fibronectin, platelets and endothelial cells under static and flow conditions.* Int. J. Med. Microbiol., 2002. **51**: p. 747-54.

112. Batoni, G., et al., *Use of antimicrobial peptides against microbial biofilms: advantages and limits.* Curr. Med. Chem., 2011. **18**(2): p. 256-79.

113. Huang, H.W. and N.E. Charron, *Understanding membrane-active antimicrobial peptides.* Q. Rev. Biophys., 2017. **50**: p. e10.

114. Wang, B.L., et al., *Fast and long-acting antibacterial properties of chitosan-Ag/polyvinylpyrrolidone nanocomposite films.* Carbohydr. Polym., 2012. **90**(1): p. 8-15.

115. Yang, K., et al., *Robust Low Friction Antibiotic Coating of Urethral Catheters Using a Catechol-Functionalized Polymeric Hydrogel Film.* Front. Mater., 2019. **6**(274).

116. Pandiselvi, K. and S. Thambidurai, *Synthesis, characterization, and antimicrobial activity of chitosan–zinc oxide/polyaniline composites.* Mater. Sci. Semicond. Process., 2015. **31**: p. 573-581.

117. Shi, S.-F., et al., *Reduced Staphylococcus aureus biofilm formation in the presence of chitosan-coated iron oxide nanoparticles.* Int. J. Nanomed., 2016. **11**: p. 6499-6506.

118. Sawai, J. and T. Yoshikawa, *Quantitative evaluation of antifungal activity of metallic oxide powders (MgO, CaO and ZnO) by an indirect conductimetric assay.* J. Appl. Microbiol., 2004. **96**(4): p. 803-9.

119. Noimark, S., et al., *The role of surfaces in catheter-associated infections.* Chem. Soc. Rev., 2009. **38**(12): p. 3435-48.

120. Silva-Dias, A., et al., *Anti-biofilm activity of low-molecular weight chitosan hydrogel against Candida species.* Med. Microbiol. Immunol., 2014. **203**(1): p. 25-33.

121. Iordache, F., et al., *Poly(lactic-co-glycolic) acid/chitosan microsphere thin films functionalized with Cinnamomi aetheroleum and magnetite nanoparticles for preventing the microbial colonization of medical surfaces.* J. Sol-Gel Sci. Technol., 2015. **73**(3): p. 679-686.

122. Visan, A., et al., *Combinatorial MAPLE deposition of antimicrobial orthopedic maps fabricated from chitosan and biomimetic apatite powders.* Int. J. Pharm., 2016. **511**(1): p. 505-515.

123. Mendoza, G., et al., *Chitosan-based coatings in the prevention of intravascular catheter-associated infections.* J. Biomater. Appl., 2018. **32**(6): p. 725-737.

124. Zhang, X., et al., *Surface immobilization of heparin and chitosan on titanium to improve hemocompatibility and antibacterial activities.* Colloids Surf. B, 2018. **172**: p. 338-345.

125. Spengler, C., et al., *Strength of bacterial adhesion on nanostructured surfaces quantified by substrate morphometry.* Nanoscale, 2019. **11**(42): p. 19713-19722.

126. Zhang, X., et al., *Quantitatively predicting bacterial adhesion using surface free energy determined with a spectrophotometric method.* Environ. Sci. Technol., 2015. **49**(10): p. 6164-71.

127. Lorenzetti, M., et al., *The influence of surface modification on bacterial adhesion to titanium-based substrates.* ACS Appl. Mater. Interfaces, 2015. **7**(3): p. 1644-51.

128. Di Ciccio, P., et al., *Biofilm formation by Staphylococcus aureus on food contact surfaces: Relationship with temperature and cell surface hydrophobicity.* Food Control, 2015. **50**: p. 930-936.

129. Ma, Y., et al., *Fabrication of super-hydrophobic film from PMMA with intrinsic water contact angle below 90°.* Polymer, 2007. **48**: p. 7455-7460.

130. Stoleru, E., et al., *Novel procedure to enhance PLA surface properties by chitosan irreversible immobilization.* Appl. Surf. Sci., 2016. **367**: p. 407-417.

131. Ang, L.F., L.Y. Por, and M.F. Yam, *Study on different molecular weights of chitosan as an immobilization matrix for a glucose biosensor.* PLoS One, 2013. **8**(8): p. e70597.

132. Oliver, J.D., *Recent findings on the viable but nonculturable state in pathogenic bacteria*. FEMS Microbiol. Rev., 2010. **34**(4): p. 415-25.

133. Phan, T.T.V., et al., *Roles of Chitosan in Green Synthesis of Metal Nanoparticles for Biomedical Applications.* Nanomaterials, 2021. **11**(2).

Appendices

Appendix A – Supplementary material regarding bacterial growth curves

In order to better understand the behavior of the selected strains and to determine the concentration of the starting cell suspensions required for biofilm assays, growth curves of *S. aureus* and *P. aeruginosa* were followed in duplicate. For this purpose, the microorganisms were inoculated in LB medium (supplemented with 1.25 $g.L^{-1}$ tetracycline solution for *P. aeruginosa*) at an initial OD at 610 nm of 0.1. The bacterial growth at 37 ˚C and 120 rpm was monitored in 250-mL shake flasks for 24 h by measuring the $OD_{610\ nm}$ and plating on agar plates (CFU estimation). The graphs $OD_{610\ nm}$ vs. t (time of incubation) and $CFU.mL^{-1}$ vs. OD_{610nm} are shown in Figures A-1 and A-2, respectively. According to Figure A-2, after resuspending the pellet in LB medium, the cellular suspensions of *S. aureus* and *P. aeruginosa* had to be adjusted to an $OD_{610\ nm}$ of about 0.1 to obtain a bacterial concentration of about 1×10^7 $CFU.mL^{-1}$.

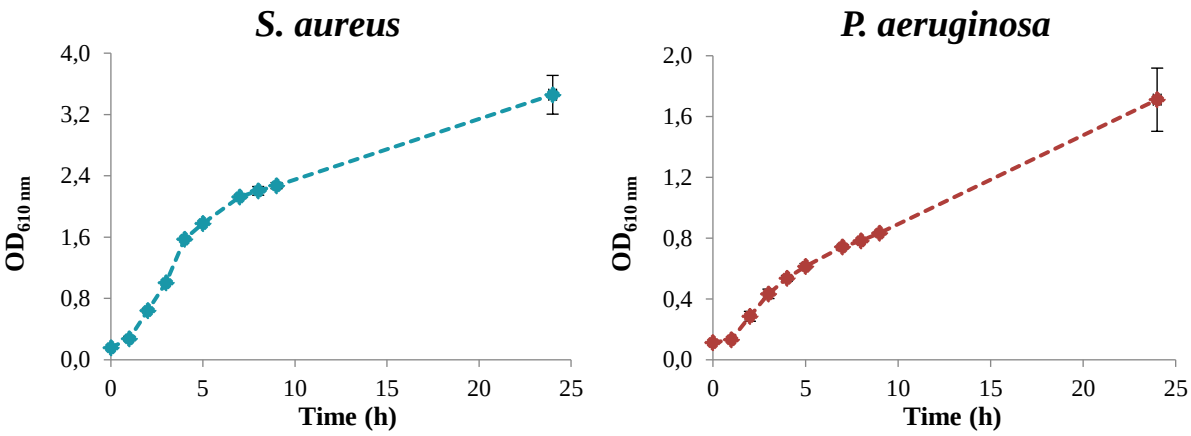


Figure A-1. Growth curves of (**a**) *S. aureus* and (**b**) *P. aeruginosa*.

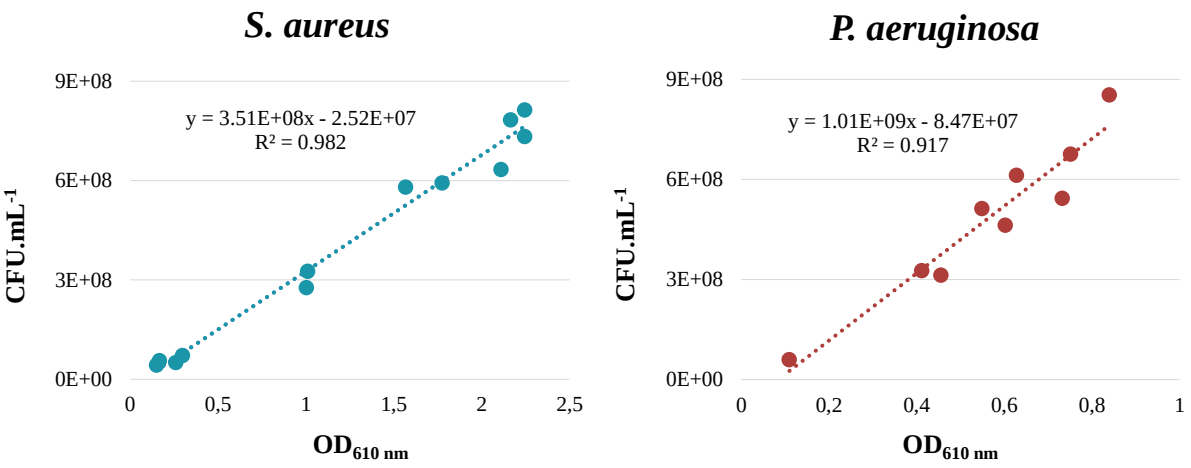


Figure A-2. Relation between $CFU.mL^{-1}$ and $OD_{610\ nm}$ for (**a**) *S. aureus* and (**b**) *P. aeruginosa*.

Appendix B – Supplementary material regarding systematic review

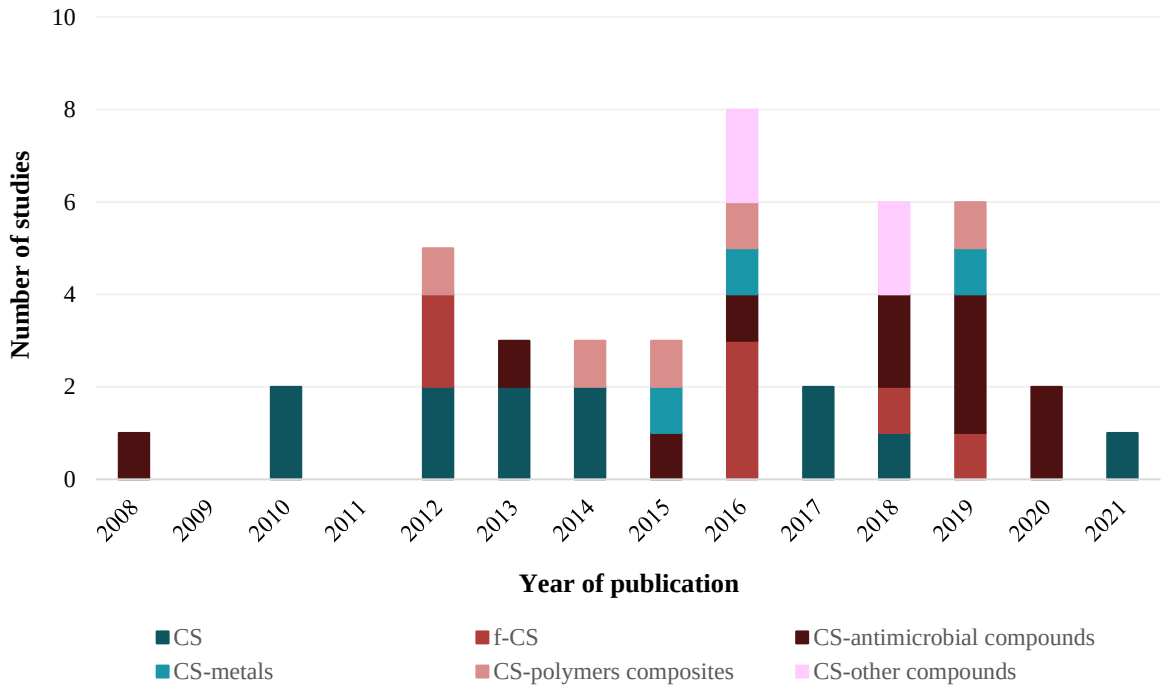


Figure B-1. Number of published studies about the anti-adhesive and/or antibiofilm activity of chitosan with application in implantable medical devices, per year.

Appendix C - Supplementary material regarding PLA and CS-coated PLA surfaces characterization

Table C-1. Water contact angles (mean ± SD) of PLA and PLA-CS films developed by dip-coating method.

Surfaces	Water contact angle values (mean ± SD)
PLA	69.53 ± 1.2
PLA-β-CS	37.01 ± 1.1
PLA-CS1	38.01 ± 5.3
PLA-CS2	38.93 ± 2.7
PLA-CS3	40.55 ± 2.8

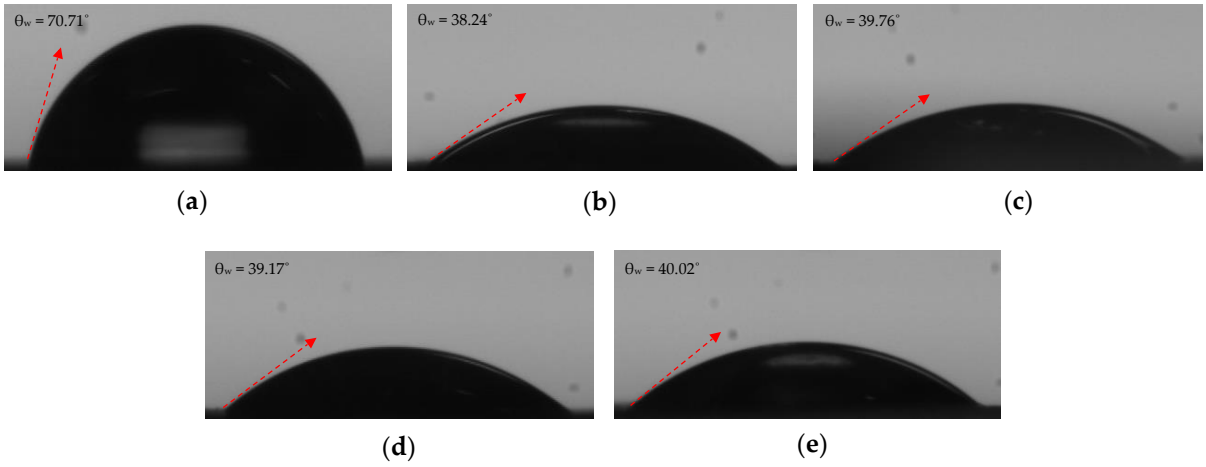


Figure C-1. Representative images of water contact angles on (**a**) PLA and CS-coated PLA surfaces: (**b**) PLA-β-CS; (**c**) PLA-CS1; (**d**) PLA-CS2; and (**d**) PLA-CS3.

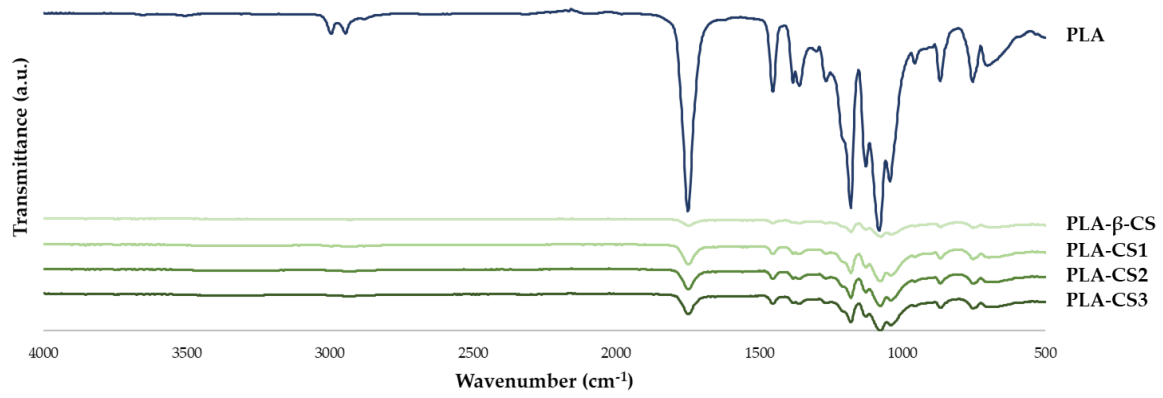
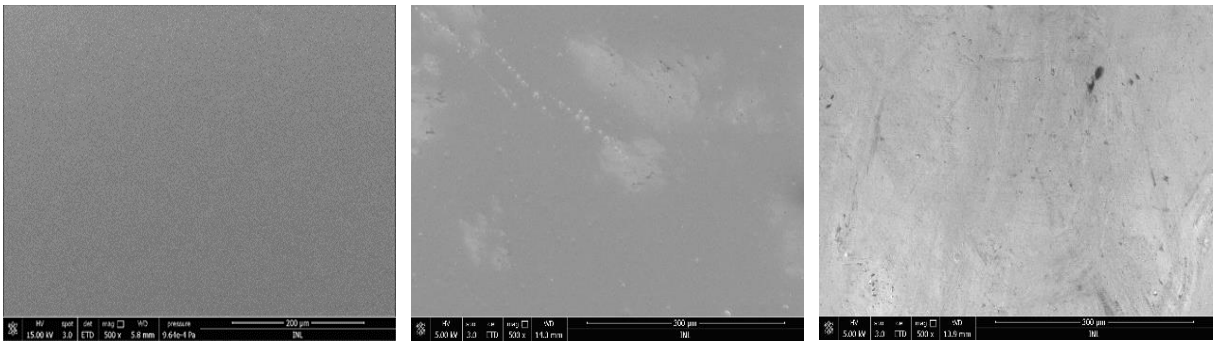


Figure C-2. FTIR spectrum of PLA films and PLA films immobilized with different samples of chitosan: β-CS, CS1, CS2, and CS3.



(**a**) (**b**) (**c**)

Figure C-3. SEM images of PLA films (**a**) and PLA films immobilized with the highest (**b,** β-CS) and lowest (**c**, CS3) molecular weight chitosan, with a magnification of 500x.

Appendix D - Supplementary material regarding the dual-species biofilms of *S. aureus* and *P. aeruginosa*

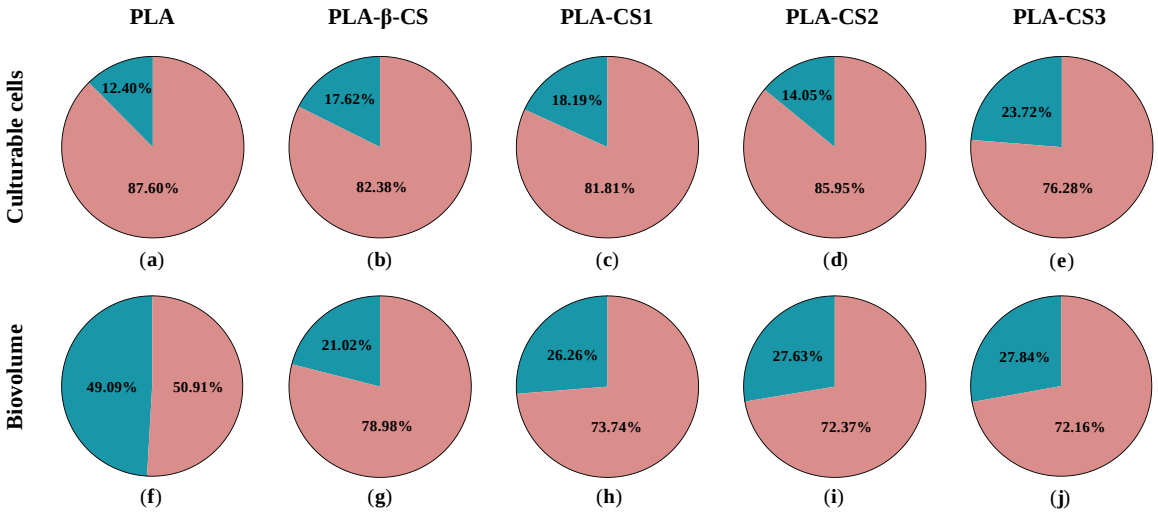


Figure D-1. Proportion of *S. aureus* (■) and *P. aeruginosa* (■) (**a-e**) culturable cells and (**f-j**) biovolume in dual-species biofilms formed on PLA and CS-coated PLA surfaces.

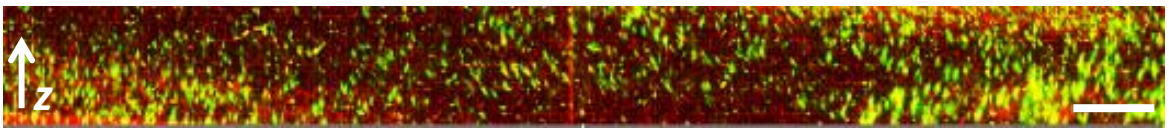


Figure D-2. Representative CLSM image of the co-localization of *P. aeruginosa* and *S. aureus* along the vertical (*z*) position in dual-species biofilms formed on CS-based surfaces. Scale bar corresponds to 50 µm.